AN ABSTRACT OF THE THESIS OF

KENNETH CARL ASH (Name) for the MASTER OF SCIENCE (Degree)

in CHEMISTRY (Major) presented on Dec 15, 1970 (Date)

Title: A STUDY OF PHOTON COUNTING EMPLOYING A DOUBLE-BEAM DIGITAL PHOTOMETER

Abstract approved: Redacted for privacy

Dr. Edward H. Piepmeier

A double-beam photometer was designed and built employing photon counting to give a direct digital readout. It was evaluated as an analytical instrument with special emphasis on pulse recovery time, pulse interaction and instrument settings. An equation is developed to explain pulse interaction in event counting systems.

A Study of Photon Counting Employing A Double-Beam Digital Photometer

by

Kenneth Carl Ash

A THESIS

submitted to

Oregon State University

in partial fulfillment of
the requirements for the
degree of

Master of Science

June 1971

APPROVED:

Redacted for privacy

Assistant Professor of Chemistry
in charge of major

Redacted for privacy

Head of Department of Chemistry

Redacted for privacy

Dean of Graduate School

Date thesis is presented Dec 15, 1970

Typed by Donna L. Olson for Kenneth Carl Ash

ACKNOWLEDGMENT

The author would like to express appreciation to Dr. Edward H. Piepmeier for his suggestions and technical assistance in the completion of this thesis. Thanks are also due to Mr. Darrell G. Petcoff for assistance with making the printed circuit boards.

TABLE OF CONTENTS

LIST OF TABLES

LIST OF FIGURES

A STUDY OF PHOTON COUNTING EMPLOYING A DOUBLE-BEAM DIGITAL PHOTOMETER

INTRODUCTION AND THEORY

Although considerable effort has been taken in improving conventional photometric instruments and their precision now approaches that of gravimetric and titrimetric methods, R. H. Muller (10) has pointed out the lack of new concepts in photometry and suggested some possible methods of improvement. Photon counting although not specifically mentioned by Muller promises to be the type of advancement that he anticipated.

The output of the anode of a photomultiplier tube consists of a discrete series of pulses due to the quantum character of light. Each pulse represents either a photon at the photocathode or less often a noise pulse initiated at one of the dynodes within the tube. An electron is ejected from the photocathode for some small number of photons striking it. The single photoelectron is amplified over a million times by a dynode chain in the photomultiplier tube. This flood of electrons provides a short current pulse which may be counted by digital circuitry. The pulse rate provides a direct measure of the radiant power falling on the detector. The pulse height will vary considerably as a result of the statistical nature of secondary electron emission from the dynodes and pulses originating at various

dynodes within the photomultiplier tube. Normally in pulse counting a discriminator level is chosen and only the pulses exceeding it counted. In this way, the extraneous noise pulses which are generally smaller are removed, increasing the signal to noise ratio. The relationship of the output pulses to incident photons has been discussed by Piepmeier (13) and Franklin et al. (6) who call this approach photon counting.

The photon arrival at the photocathode may be considered random (6) and therefore the pulse output of the photomultiplier tube will be random. Each pulse has a finite duration due to the response time of the electronic detection system and differences in the path lengths taken by the electrons in the pulse within the photomultiplier. Each pulse leaves the detection system insensitive for a short but finite dead time during which no events are detected. This causes some error in the pulse counting but this phenomena has been studied in depth (7) and statistical methods of dealing with it developed (14). Later in this paper partial compensation for pulse loss will be discussed.

At higher light intensities, the pulse rate becomes such that large numbers of pulses become superimposed upon one another. The result is a loss in the digital character of the signal. This is the case in a conventional photometer where the current pulses are averaged or integrated by slowly responding electronics to produce a

relatively constant current.

The classical photometer employs both relatively high light intensities and a large current-sampling anode resistance. The voltage drop due to the anode current is amplified and measured as an analog signal. The measuring device is generally a voltmeter, graduated to give a numerical readout. In order to obtain reasonable accuracy with this method, highly stable amplifiers and power supplies must be used. There is considerable room for error to occur in this digital-to-analog-to-digital conversion.

A direct pulse counting system as first discussed by Ross (16) has been suggested as superior to the conventional method especially at low light intensities (11). The number of pulses counted is taken as a direct digital result thus eliminating several possible sources of error. The main advantage of photon counting spectrophotometers over conventional photometers is increased accuracy and precision, especially at low light intensities (13). The photon counting spectrophotometer is also simpler and less expensive to construct since it does not require extremely stable power supplies and amplifiers as will be shown later.

The double-beam ratio method used in this photometer employs two similar light detection and pulse counting systems. The sample beam pulse counting system activates a digital readout which reports the number of pulses counted. The reference beam counting system

activates a gate which stops both counting systems when a preselected number of pulses has been counted. This system significantly increases stability over a single beam system (10).

If a blank is introduced into the reference cell and a sample into the sample cell, the readout will be a measure of the transmittance of the sample. If the blank is introduced into the sample cell and the sample into the reference cell, the readout will be a measure of the reciprocal of the transmittance of the sample. This comes about because the sample is now absorbing light in the reference beam causing a longer counting period.

To give an example, suppose that the sample and reference beams are matched and a blank solution is placed in each cell. If the reference beam detecting system is set at 100×10^3 counts, the sample beam detection system will register 100×10^3 pulses indicating a sample transmittance of one (100%) based on a transmittance of one for the reference sample. The reciprocal transmittance in this case is also one as shown below.

$$1/T = 1.00/1.00 = 1.00. \qquad (1)$$

Now consider that a sample having a transmittance of 0.50 is placed in the sample cell. The sample will transmit one half of the impinging radiation and the detection system will register 50×10^3 pulses indicating a transmittance of 0.50 (50%). The same sample

placed in the reference beam (with the blank now in the sample beam) will absorb one half the impinging photons causing the reference detection system to take twice as long to receive 100×10^3 pulses. The sample detection system will also operate twice as long and therefore registers twice as many pulses or 200×10^3, corresponding to a reciprocal transmittance of two.

$$1/T = 2.00/1.00 = 2.00 \qquad (2)$$

EXPERIMENTAL

Instrumentation

A block diagram of the double-beam digital photometer built for this study is shown in Figure 1.

Light Source

The light source used was a Westinghouse WL22601 neon-filled calcium hollow-cathode tube. It was powered by a Heathkit EUW-15 regulated power supply.

The current was measured with an ammeter having full scale ranges of 0.2, 2.0 and 20.0 milliamperes, selected by means of a rotary switch. The rotary switch was also wired to select an appropriate series resistance for the light source, thus protecting the hollow cathode tube and the ammeter from accidental overload. The power supply voltage regulator and a Heathkit EUW-28 resistance substitution box in series with the hollow cathode allowed a current range of from one microampere to twenty milliamperes.

A 421 nm interference filter with an 11 nm bandpass and an ultraviolet broad band filter which cuts off above 400 nm were used together to isolate a narrow band of neon lines between 331 and 360 nm (13). This wavelength is near the maximum response region of the photomultiplier tubes used.

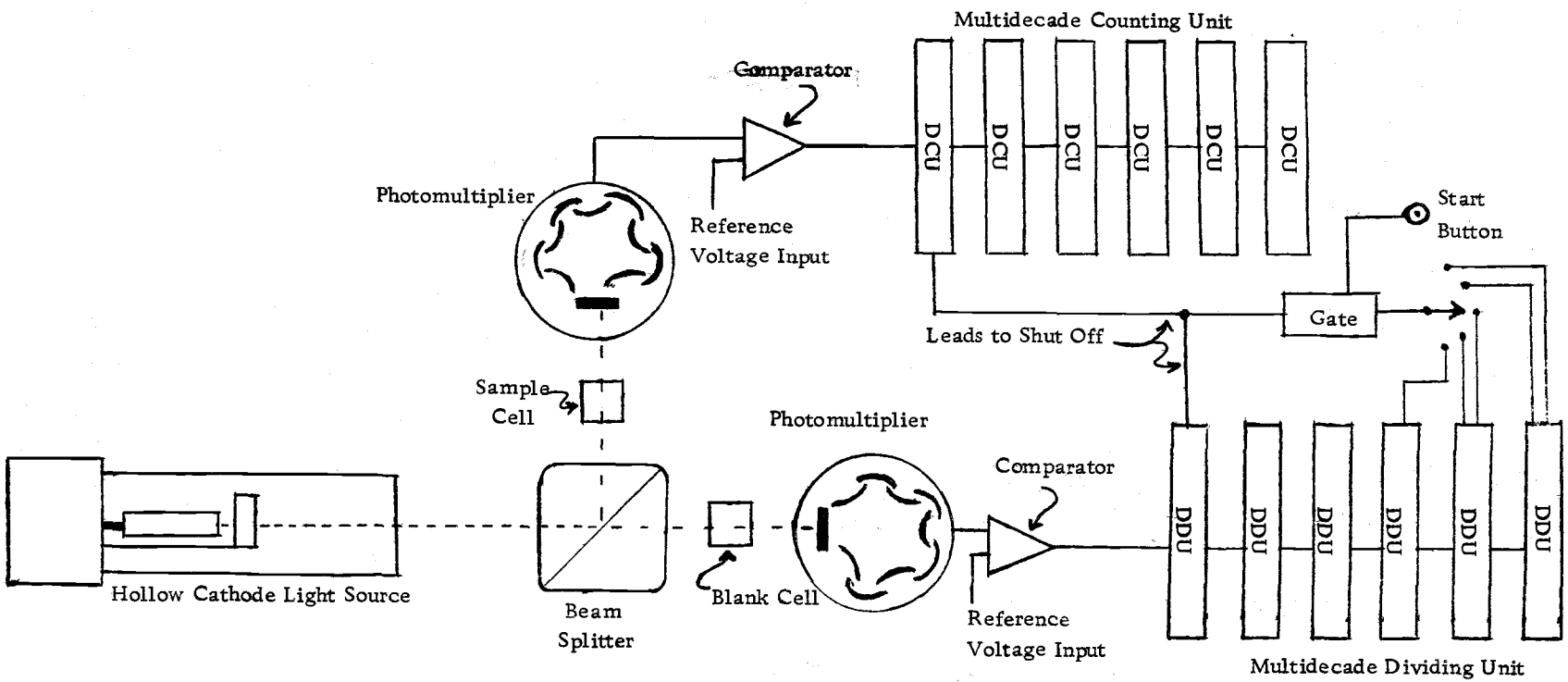

Figure 1. Block diagram of photometer.

An alternate light source used was a General Electric PR3, 4.5-volt Tungsten bulb. It was powered by a type CRF-19017, 12-volt wet cell battery tapped to supply four volts. A Heathkit EUW-28 resistance substitution box was placed in series with the bulb in order to control the bulb voltage.

Some work was also done using a McKee-Pederson 1018 Monochromator and a 6-volt MP-1019 tungsten light source. The tungsten bulb was powered by a Sorenson QSB6-8 power supply. The monochromator was attached to the front of the photometer and a front surface mirror used to direct the beam onto the beam splitter.

Optic and Sample System

A 33 x 33 x 20 mm prism type beam splitter provided by Edmund Scientific was used. The sample and reference cells were Beckman 1-cm path length glass cells. An adjustable slit was placed in the sample beam between the cell and the photomultiplier.

Light Detection System

The light detectors, Figure 2, were RCA-1P28 photomultiplier tubes. The approximate response range of the 1P28 is from 200 to 600 nm with the maximum near 340 nm (15). Operating potential was supplied by a Hewlett Packard-Harrison 6515A dc power supply. The dynode potentials for both beams were maintained by a series of

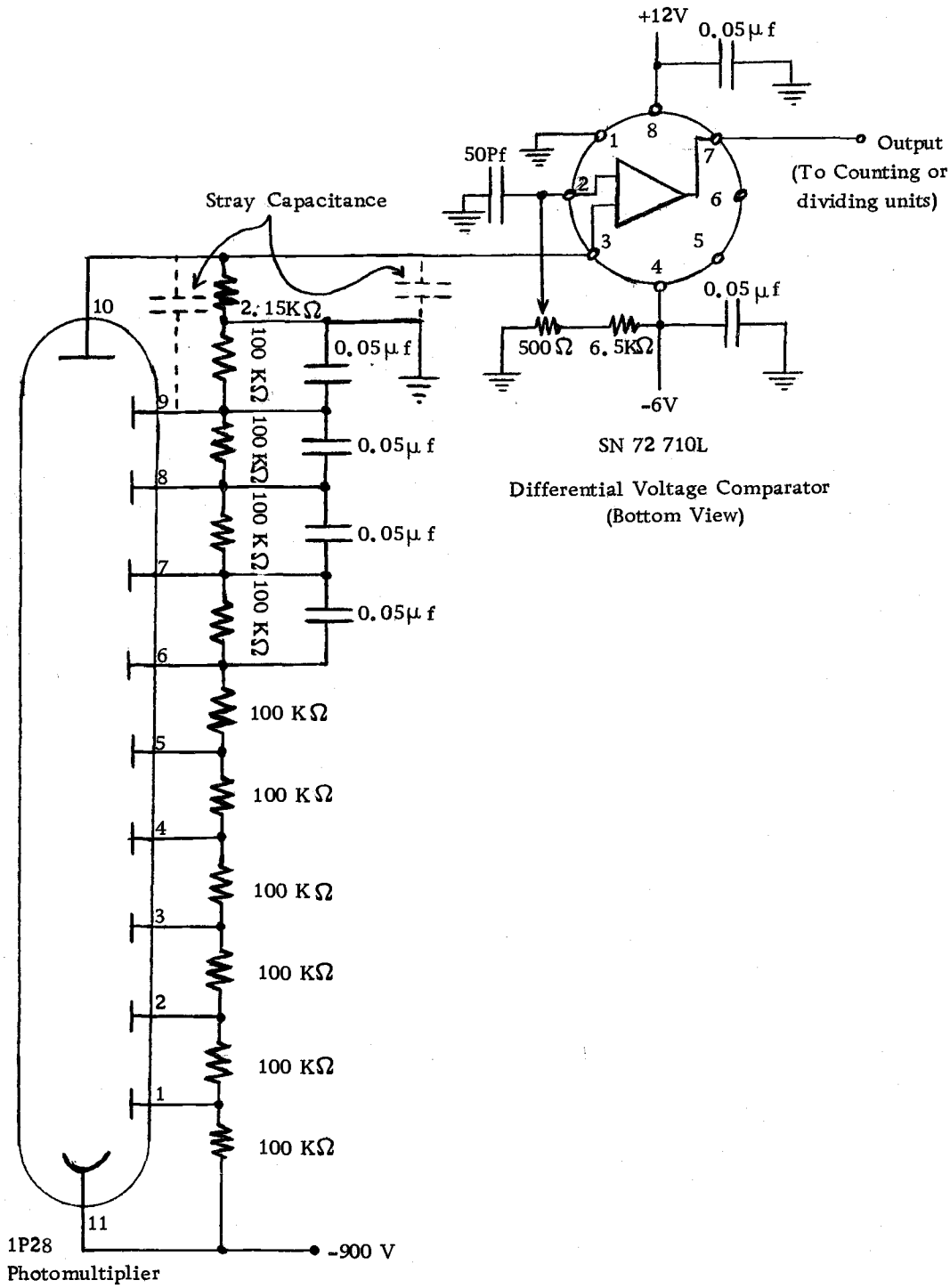

Figure 2. Light detection system.

one-percent 100-kilohm resistors. Four 0.05-microfarad ceramic capacitors were wired in parallel with the last four resistors of each photomultiplier to maintain constant dynode potential during the current pulses. A one-percent, 2.15-kilohm resistor was used for the anode lead resistance. The dashed line capacitors indicate stray capacitance in the system.

Texas Instruments SN72710L high speed differential voltage comparators were used as pulse height discriminators and amplifiers. A stabilized Heathkit EUW-17 transisterized power supply provided the 12-volt potential. The negative 6-volt potential was provided by a Heathkit 1P-27 regulated low voltage power supply. The reference voltage was tapped from the negative 6-volt lead through a voltage divider. The comparator power leads were decoupled with 0.05-microfarad ceramic capacitors and the reference voltage leads were decoupled with 50-picofarad ceramic capacitors. The comparators and wiring were shielded with aluminum foil.

It was found that further amplification of the photomultiplier signal was not necessary. This simplified the light detecting system. Some work in this area has also been done by Akins (1).

The photomultiplier output is not a continuous current or potential across the anode resistor but a series of varying pulses. There is also a small residual voltage at the photomultiplier anode upon which the pulses are superimposed. The sum of the residual voltage

plus the pulse voltage must be kept low enough to avoid damage to the discriminator.

The greatest current which the photomultiplier as wired could develop for any length of time beyond that necessary to discharge the capacitors is given approximately by the relation:

$$I_{max} = E/R = \frac{90}{1.0 \times 10^{5}} = 9.0 \times 10^{-4} \text{ amp.} \qquad (3)$$

where E = the voltage drop and R = the resistance between two dynodes. The output current however could not approach this value or the current drain would lower the dynode potentials and decrease the gain of the photomultiplier.

The maximum average anode potential for a 2.15-kilohm anode resistor can be calculated from the maximum current for the circuit in Figure 2 by the equation:

$$E_{max} = I_{max} R_{anode} = (9.0 \times 10^{-4})(2.15 \times 10^{3}) = 1.9 \text{ volts} \qquad (4)$$

This is well within the ± 7 volt absolute maximum input voltage for the AN7271OL comparator(5) since few pulses have a height in excess of 0.2 volts.

The accumulation of a large number of counts during a measuring period is desirable because random counting error is reduced and a more accurate value obtained. In order to save time and reduce the

influence of background a fast count rate is desirable. A fast count rate necessitates a short dead time so that relatively few pulses will overlap and be lost.

The dead time can be shortened by reducing the anode resistance, but below 2 kilohms this was observed to decrease the pulse height making the setting of the discriminator more critical.

Multidecade Dividing Unit

The multidecade dividing unit (MDU) shown in Figure 3, is based on Lancaster's electronic stopwatch design (9). The MC 724P, MC 776P and MC 790P integrated circuits were made by Motorola. The MDU was mounted on two printed circuit boards, shown in Figure 4. The integrated circuits and wiring are on top of the circuit boards but are pictured as they would appear from the bottom so as not to reverse the boards.

The MDU consists of six decade dividing units. It is tapped in five places by a rotary switch, providing division by 1×10^6, 4×10^5, 1×10^5, 4×10^4 and 1×10^4.

The MC 724P quadruple two input gate is connected by a bistable multivibrator such that a potential applied to the "stop" lead produces an output signal at the "shutoff" lead. The "shutoff" lead is connected to pin 3 of the first flip-flop in both the MDU and the multidecade counting unit. The signal switches the flip-flops to the set

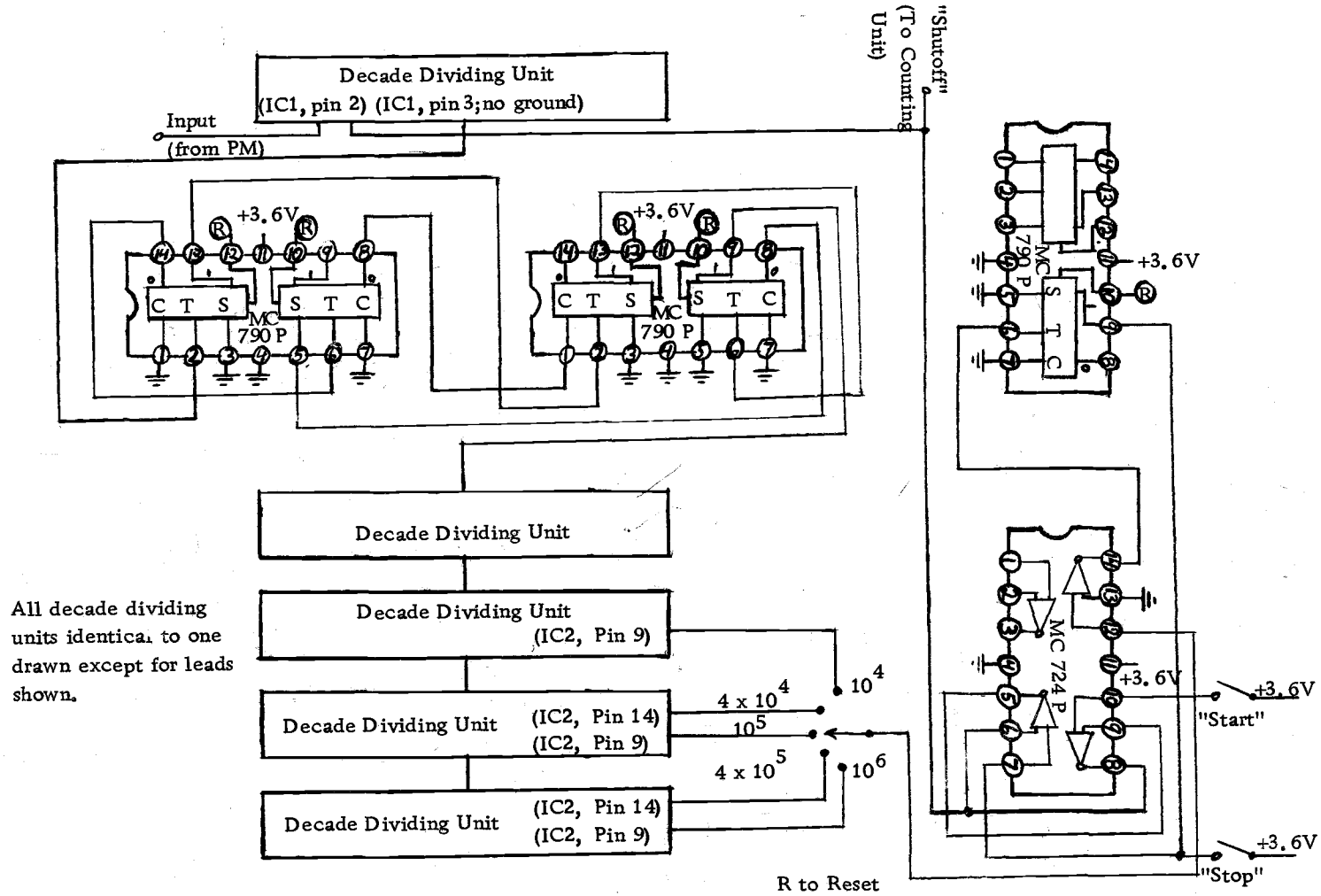

All decade dividing units identical to one drawn except for leads shown.

Figure 3. Multidecade dividing unit.

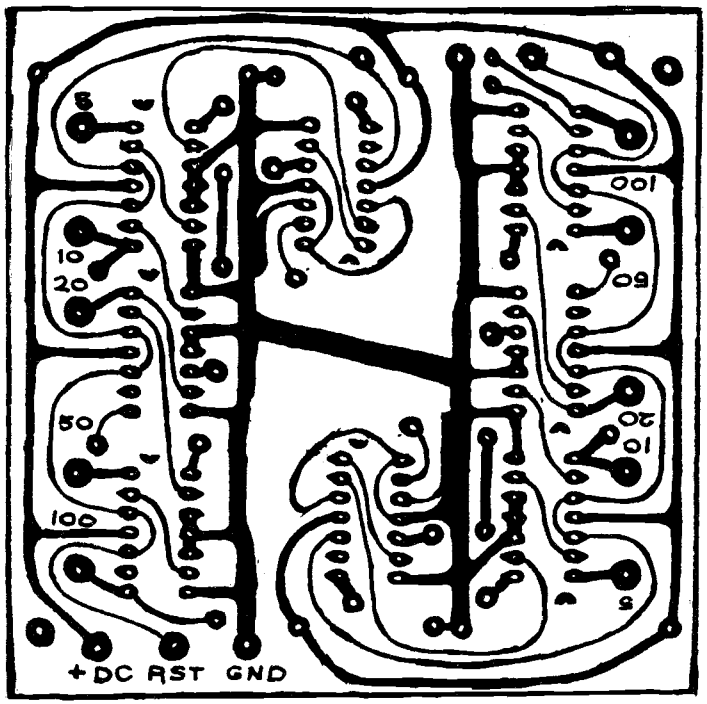

Actual Size

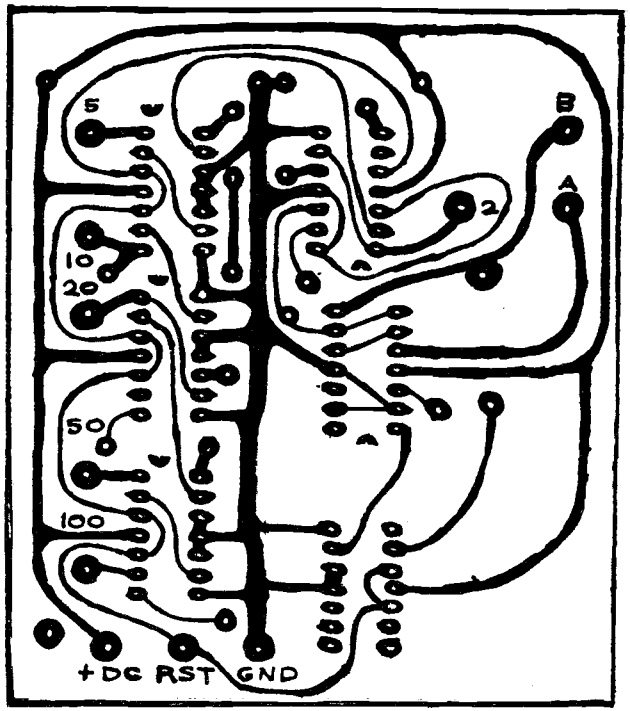

Actual Size

Figure 4. Dividing unit printed circuit.

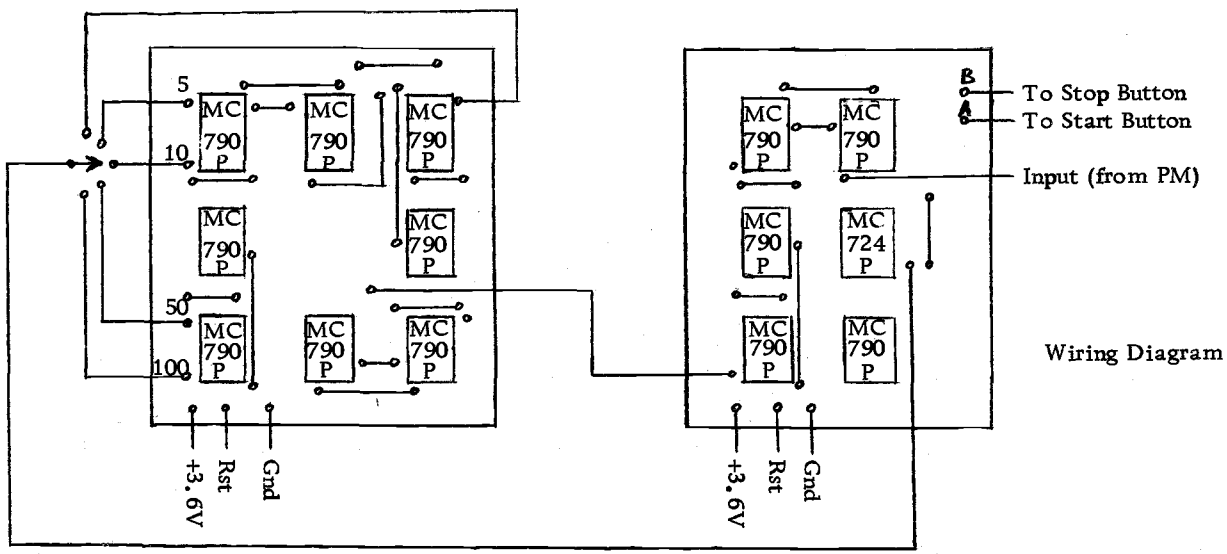

Figure 4A. Dividing unit printed circuit wiring diagram.

position thus stopping the counting and dividing units and holds them there.

A potential applied at the "start" lead of the multivibrator flips it so that no output signal is produced and the counting and dividing units may begin operating. The units continue counting until the MDU accumulates the number of pulses set by the rotary switch. The MDU then emits a pulse which is inverted and triggers a flip-flop which supplies a potential to the "stop" lead of the multivibrator.

A single decade dividing unit consists of two integrated circuits each containing two flip-flops. The logic table for the dividing unit is shown below.

Table 1. Decade logic table.

Pulse Number	State of flip-flop #1	State of flip-flop #2	State of flip-flop #3	State of flip-flop #4
0	0	0	0	0
1	1	1	0	0
2	0	1	1	0
3	1	1	1	0
4	0	1	0	1
5	1	0	0	1
6	0	0	0	1
7	1	1	0	1
8	0	1	1	1
9	1	0	1	1
10	0	0	0	0

The flip-flops are numbered from left to right as drawn in the schematic. The "0" and "1" states are also designated as drawn in the schematic.

Multidecade Counting Unit (MCU)

The multidecade counting unit (MCU) used is a modification of Lancaster's decimal counting unit (DCU) and is similar in logic to the dividing unit (8). The schematic of the modified counter is shown in Figure 5. The 2N5129 transistors were obtained from Fairchild. The lamps are Grain of Wheat No. 10 bulbs obtained from Aristo-Craft, Newark, New Jersey. The counters were mounted on printed circuit boards, shown in Figure 6.

The counting and dividing units were powered by a Heathkit Regulated Low Voltage Power Supply, model 1P-27. Each counting unit draws a current of 190 milliamperes, 80 milliamperes of which is used by the bulb. Six counting units were connected in series, giving a capability of 999,999 counts.

The operating and reset potential for both counting and dividing units is 3.6 volts; the reset is connected through a momentary switch. The power supply need not be especially stable as will be shown later in this paper. Batteries could be used if a portable instrument is desired. The counting and dividing units will operate at frequencies greater than ten megahertz and have no lower frequency limit.

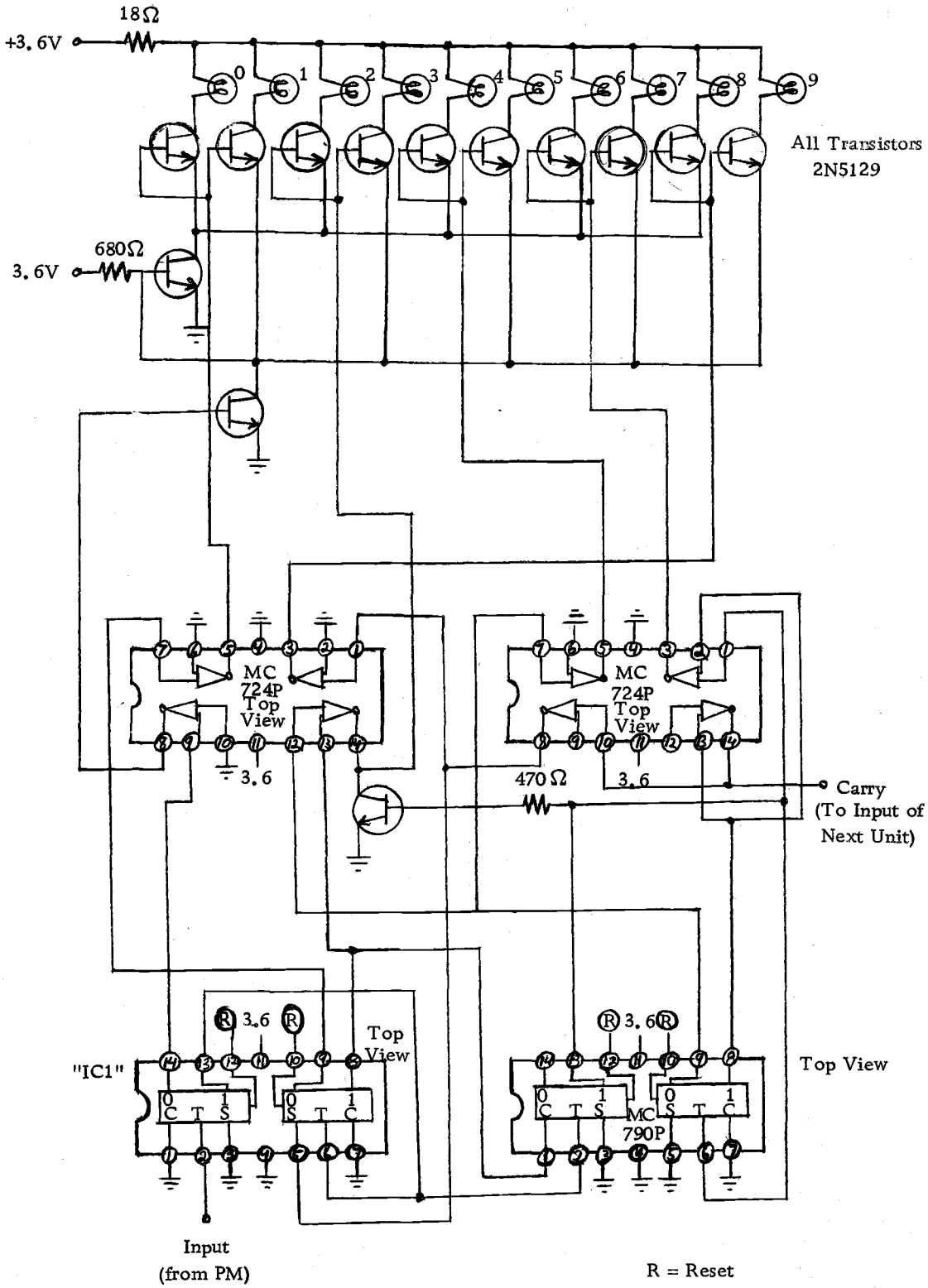

Figure 5. Decade counting unit.

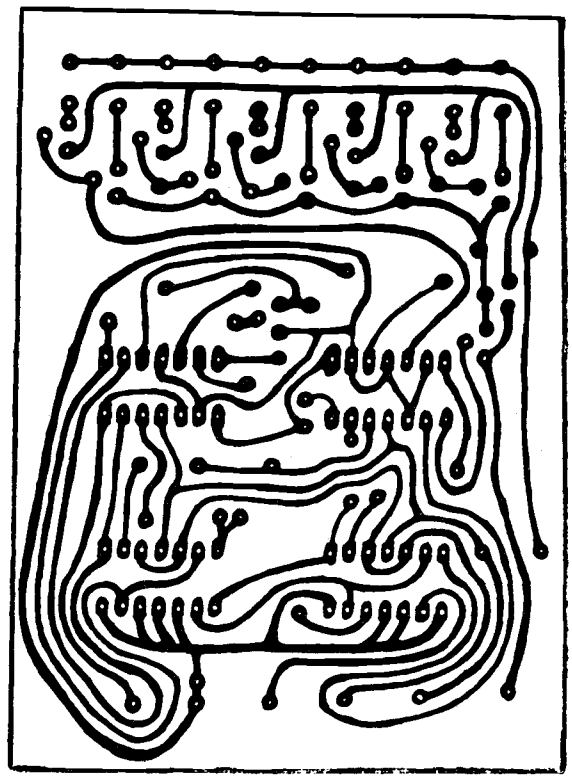

Actual Size

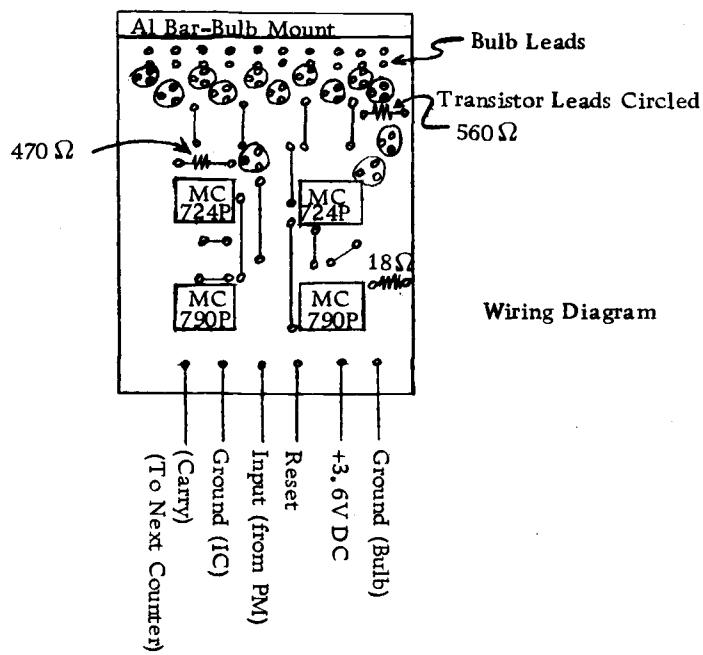

Figure 6. Decade counting unit printed circuit.

An automatic switch was employed to turn on the readout lights after the counting had ceased, thus prolonging lamp life. This switch is not necessary and was not included in the schematic.

Instrument Design

The actual instrument design in shown in Figure 7. The light detection system is mounted on one board. The electrical connections to other sections of the instrument are made through banana plugs. This insures easy removal of the detection system and allows a simple method of making connections to the counting and timing units. A door in the case beneath the detection system provides easy access to the wiring and banana plug connections.

The multidecade dividing unit was wired on two printed circuits mounted together on a board and connected with banana plugs so as to make the unit easily removable. The individual decade units are also removable, and their electrical connections employ octal plugs and sockets.

The case was built of 3/4 inch plywood; all edges of the light tight section were beveled. All permanent joints were glued, fastened with wood screws and covered with black tape. The beveled edges of the front, top and inside compartment divider were covered with black felt. The compartment divider was fastened with six wood screws and the front with nine. They were not glued. The top of the light tight

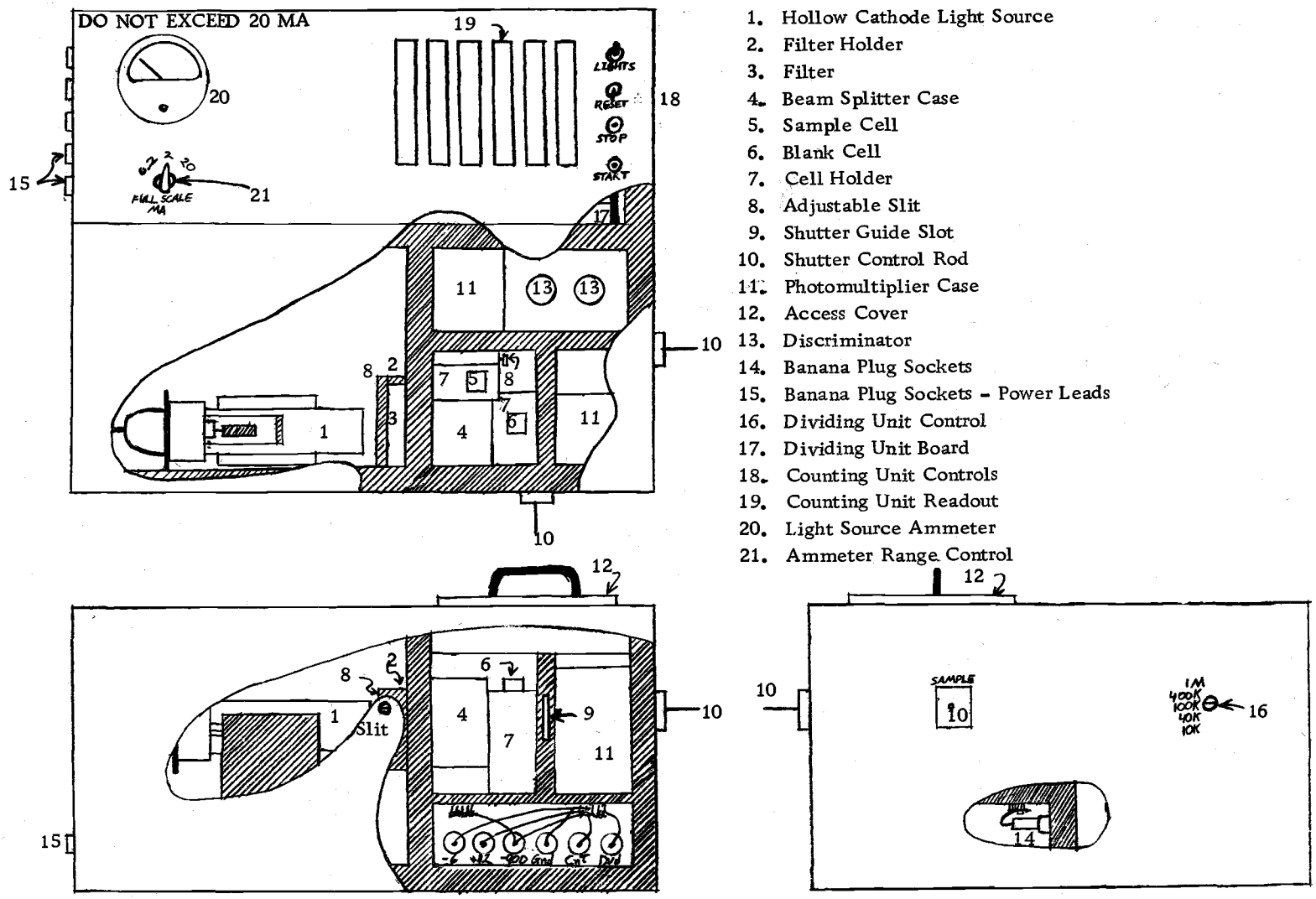

1. Hollow Cathode Light Source
2. Filter Holder
3. Filter
4. Beam Splitter Case
5. Sample Cell
6. Blank Cell
7. Cell Holder
8. Adjustable Slit
9. Shutter Guide Slot
10. Shutter Control Rod
11. Photomultiplier Case
12. Access Cover
13. Discriminator
14. Banana Plug Sockets
15. Banana Plug Sockets - Power Leads
16. Dividing Unit Control
17. Dividing Unit Board
18. Counting Unit Controls
19. Counting Unit Readout
20. Light Source Ammeter
21. Ammeter Range Control

Figure 7. Instrument design - 1/5 scale.

section was secured by means of six wingnuts (not shown in Figure 7). The sample access cover was double beveled and the edges covered with black felt. The shutter control rods were light sealed with black felt and two rubber seals each, one inside and one outside the box. All wire leads into the light tight section were sealed with wood putty and covered with 1/8 inch fiberboard. The bottom access door was fastened by wood screws and sealed with black tape. The shutters were 1/16 inch black metal plates, sliding in slots covered on both sides with black felt. The beam splitter case is a 2 x 1-3/4 x 1-1/2 inch aluminum utility box and the photomultiplier cases are 4 x 2-1/2 x 2-1/2 inch aluminum utility boxes. The interior of the case was painted flat black.

The top and back covers of the electronics section were unbeveled 1/4 inch plywood fastened by wingnuts. All power supplies were external and connected through banana plug sockets set in the outer case wall although the case is large enough to contain an internal power supply if desired. The supply voltages were set and monitored with a Fairchild Model 7050 Multimeter.

Reagents

The chemical system studied was potassium dichromate in 0.64 M nitric acid. Deionized, distilled water and reagent grade potassium dichromate and nitric acid were used.

An acidic potassium dichromate system was chosen because it absorbs strongly in the 330 to 360 nm range of the light source. The solutions were made acidic to prevent conversion of the dichromate to chromate ion. Nitric acid was used as other common strong acids complex with the dichromate ion (3).

A potassium permanganate solution in distilled, deionized water was also used for part of the work.

Procedure

The photometer was allowed to warm up for one to two hours before use. The hollow cathode light source was allowed twenty minutes to stabilize whenever its current was changed.

The sample and reference cells were not removed during analysis in order to insure stability of position. Sample solutions were introduced by means of a syringe and removed with a vacuum suction system both having teflon needles.

The sample and reference outputs were matched to equal count rate with the adjustable slit in the sample beam. This was necessary because the photomultipliers, dynode resistors and beam intensities were not perfectly matched.

The light intensity was changed by means of a variable slit between the light source and the filter. The intensity can also be changed by changing the hollow cathode current but this changes the

spectral character of the light. At low currents the neon lines predominate, but at higher currents the calcium lines become more and more prevalent. Since the filters are not ideal, an increasing proportion of the 423-nm calcium line will be present at higher currents where cathode sputtering becomes significant. For this reason the hollow cathode current was kept as low as possible.

The observed count rates of the reference beam were determined by introducing a 100-kilhertz square wave into the counting or dividing unit with a Heathkit EUW-27 sine-square generator. Such modifications are easily made with the banana plug connections mentioned earlier. The complete beam count rate could then be matched to the reference beam using the adjustable slit.

If a 100-kilohertz square wave is introduced into the counting unit and the output of one of the photomultipliers into the dividing unit, the dividing unit shuts off the counter at the predetermined number of pulses as set by the rotary switch, usually 10^6, and the readout records counting time in seconds times 10^5. Simply dividing 10^6 by the counting time gives the counting rate. If the square wave is introduced into the dividing unit and the photomultiplier output is fed into the counting unit, a divider setting of 10^5 gives a readout directly in pulses per second.

To find the true count rate the overlapping pulses must be taken into account. True count rates were determined by two methods. The

simplest method, the simulated light intensity method, employs the photometer as a single beam instrument with a sine-square generator connected to the dividing unit in place of the reference beam output. Varying the divider setting and the square wave frequency allowed counting periods from 0.01 to 5×10^4 sec.

The observed count rate was recorded at various incident light intensities both with and without an absorbing sample in the light beam. The results were graphed as the count rate with no absorbing sample against the count rate with the absorbing sample in place. The count rate with no absorber was chosen as the ordinate. A sample cell containing a dichromate solution with an absorbance of at least one (10% transmittance) was used throughout for the absorber. The cell was removed to measure the count rate with no absorber. The light intensity was varied with an adjustable slit. When the absorbance is large, the count rate with the absorber in place will be low and can be considered proportional to the relative light intensity to a very good approximation since little pulse overlap takes place. The graph shows the change in the observed count rate (n), plotted on the ordinate, with the relative light intensity, plotted on the abscissa. An extension of the straight part of the plot shows the actual count rate (N) on the ordinate vs the relative light intensity. The values of n and N at any chosen light intensity can be obtained from the graph and used to calculate the dead time by the equations 14 and 16 reported in the

Appendix.

A second method, the transmittance method, can employ the photometer as either a single or double beam instrument. In this method, the transmittance of an absorbing sample is plotted against the count rate without the absorbing sample for different light intensities. Values of n_o and N_o can be determined from the graph with the relationship developed below.

The transmittance of the absorber is given by:

$$T = I/I_o = N/N_o \tag{5}$$

where T = true transmittance,

I = intensity of the transmitted light,

I_o = intensity of the incident light,

N = true count rate with absorber,

N_o = true count rate without absorber.

The observed transmittance is given by:

$$T_{obs} = n/n_o \tag{6}$$

where t_{obs} = observed transmittance,

n = observed count rate with absorber,

n_o = observed count rate without absorber.

Count loss due to the dead time is much more pronounced at higher count rates, therefore the loss for N_o will be greater than for

N. Since the absorber was chosen such that N_o is ten times larger, the ratio n/n_o will increase as the light intensity increases. This change in observed transmittance with count rate allows the calculation of N_o.

The development of the relationship between the actual and observed count rates is shown below. Since,

$$\frac{T_{obs}}{T} = \frac{n/n_o}{N/N_o} \tag{7}$$

it follows that

$$\frac{T_{obs}}{T} = \frac{nN_o}{Nn_o} \tag{8}$$

If the absorbance is large enough that n is relatively small the pulse overlap for n is negligible and approximately equal to N, the equation becomes

$$\frac{T_{obs}}{T} = \frac{NN_o}{Nn_o} = \frac{N_o}{n_o} \tag{9}$$

which can be rearranged to

$$n_o \left(\frac{T_{obs}}{T} \right) = N_o \tag{10}$$

At very low light intensities, T_{obs} becomes very nearly T and the equation becomes

$$n_o \left(\frac{T_{obs}}{T_{obs1}} \right) = N_o \qquad (11)$$

where T_{obs1} = observed transmittance at low light intensity. These values of n_o and N_o can be used to calculate the approximate dead time with either equation shown below:

$$\tau = (N-n)/nN \quad \text{or} \qquad (12a)$$

$$\tau = [\ln(N/n)]/N \qquad (12b)$$

These equations are developed and explained in the Appendix.

RESULTS AND DISCUSSION

Power Supply Stability

The deviation in counting rate with a change in the counter operation voltage for the sample beam used as a single beam photometer is shown in Figure 8. The discriminator voltage was set at 0.064 volts. The normal counter voltage is 3.60 volts. Figure 8 shows that an unstable power supply fluctuating between 3.5 and 3.7 volts, a change of 5.5% would cause a change of less than $\pm$ 0.25% in count rate. This is also the case for double beam operation since both counters are used for single beam as well as double beam operation.

Figures 9 and 10 show the counting rate deviation with the comparator operating voltages. A fluctuation of $\pm$ 0.1 volt (0.8%) in the positive 12-volt supply can cause a deviation of up to $\pm$ 0.5% in the counting rate. A fluctuation of $\pm$ 0.1 volt (1.6%) in the negative 6-volt supply can cause a counting rate deviation of $\pm$ 1.0%.

In a double beam photometer, the deviation in the sample and reference beams would be expected to cancel giving a much smaller error in the result. Table 2 shows the deviation inherent in the double beam photometer with fluctuations in the positive 12-volt power supply. Deviation is reported in percent change from output at normal voltage setting. This deviation is within the random counting error of

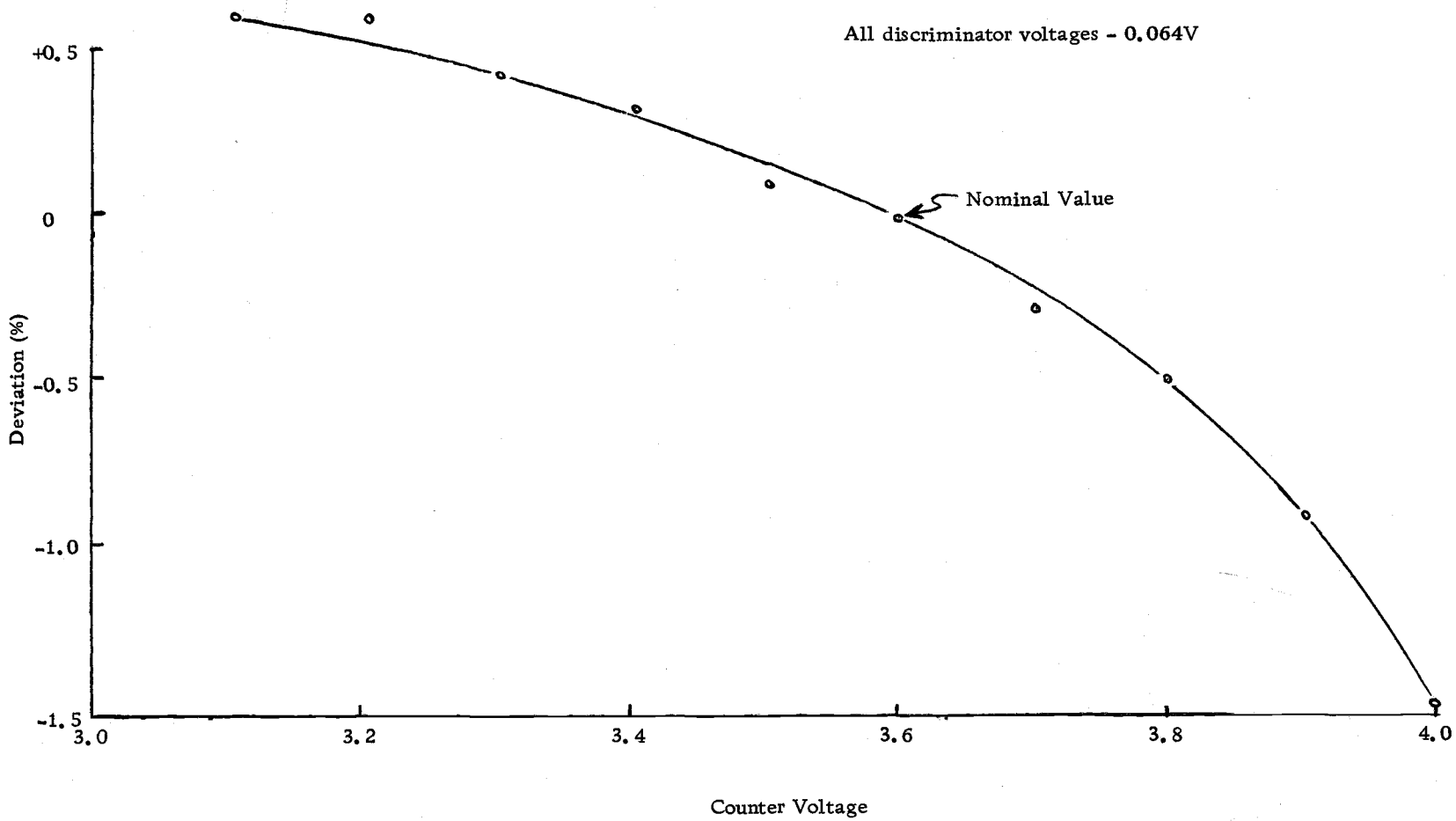

Figure 8. Counting rate deviation vs. counting unit voltage for single beam.

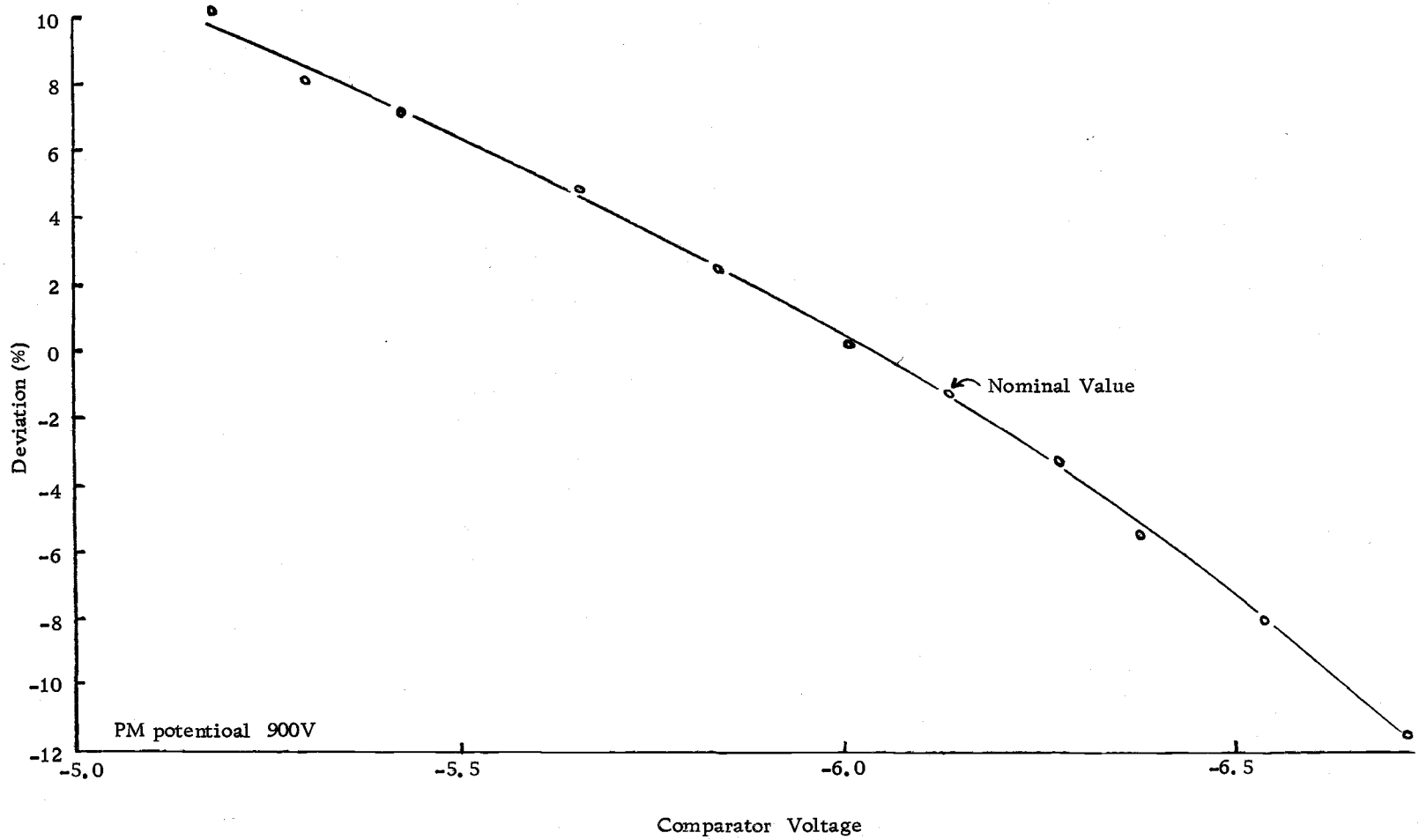

Figure 9. Counting rate deviation vs. negative comparator voltage for single beam.

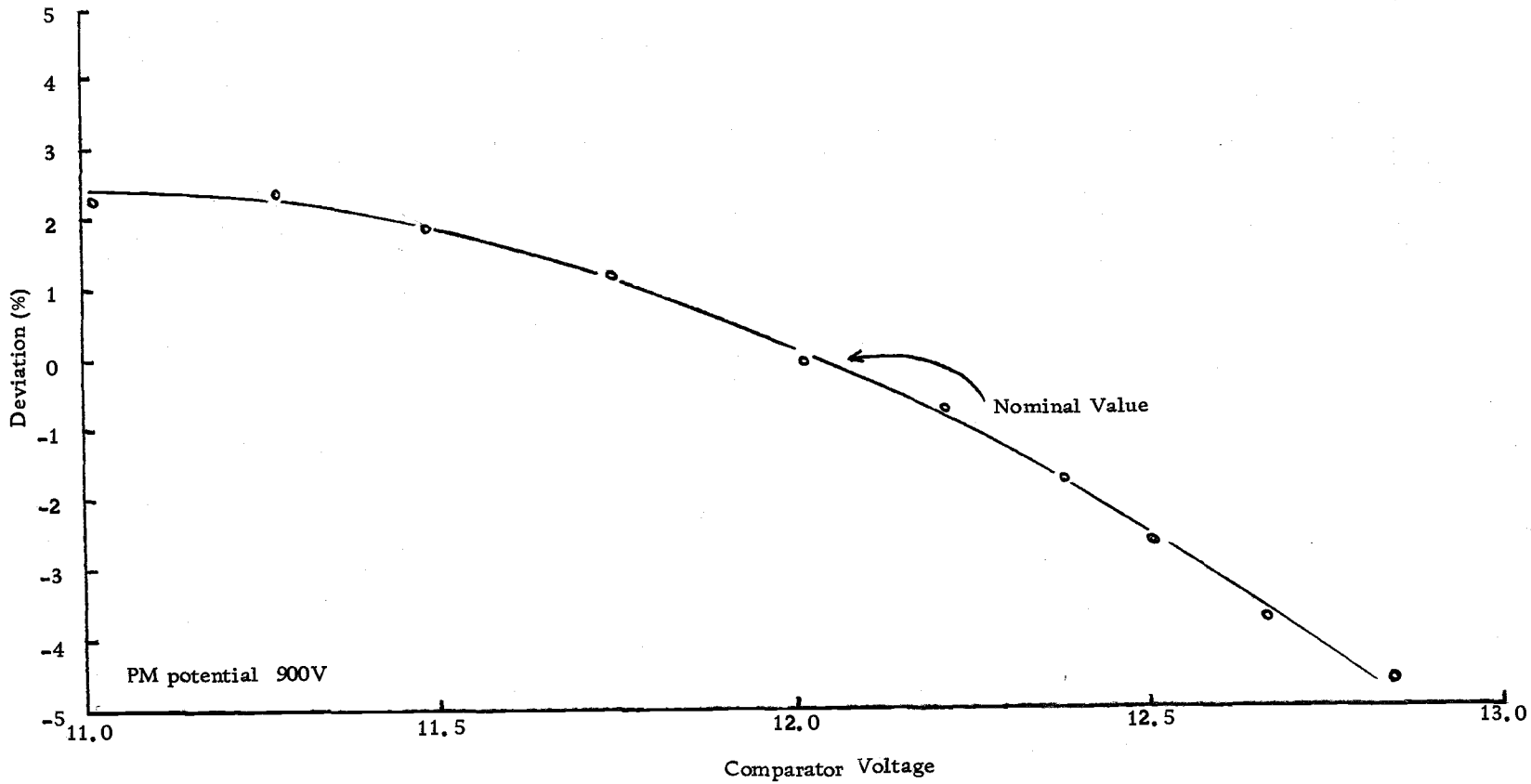

Figure 10. Counting rate deviation vs. positive comparator voltage for single beam.

the system.

Table 2. Power supply instability error for the double beam 12-volt discriminator supply.

Positive discriminator potential (V)	Count rate deviation (%)
12.15	-0.01
12.07	+0.05
12.00	0.00
11.93	+0.01
11.85	+0.10

A fluctuation in the negative 6-volt discriminator power causes a greater error, probably due to changes in the threshold levels which are difficult to match for the two beams. The results are presented in Table 3. The negative 6-volt setting was arbitrarily defined as zero error.

Table 3. Power supply instability error for the double beam negative 6-volt discriminator supply.

Negative discriminator potential (V)	Count rate deviation (%)
-6.15	-1.25
-6.10	-0.57
-6.05	-0.15
-6.00	0.00
-5.95	+0.26
-5.90	+0.54
-5.85	+0.81

The measurements for Figures 8, 9 and 10 and Tables 2 and 3 were obtained by adjusting the power supplies. A rapid fluctuation in the power would have less effect on the count rate because of the averaging effect, especially if the supply were properly decoupled.

Highly stable power supplies need not be used for the 12-volt discriminator supplies and the counting and dividing units, especially if the power leads are decoupled to even out rapid fluctuations. A moderately stable negative 6-volt power supply is needed.

The photomultiplier potential for a single beam instrument must be rather stable since an increase in the potential will increase the gain of the photomultiplier tube and thus increase the fraction of pulses exceeding the discriminator voltage. This precaution is not necessary if a double beam instrument is used.

The variation of count rate with photomultiplier potential for single beam operation is shown in Figure 11. The hollow cathode light source was used at a current of one ma. As the voltage is increased, the counting rate approaches a plateau. (One thousand volts was set as a maximum limit to avoid damage to the photomultiplier.) The plateau is approached sooner at lower threshold levels. Unfortunately, low discriminator voltages and high photomultiplier potentials give high background counts. Some work should be done with other photomultipliers which may provide a more suitable plateau.

Double-beam operation greatly reduces error due to

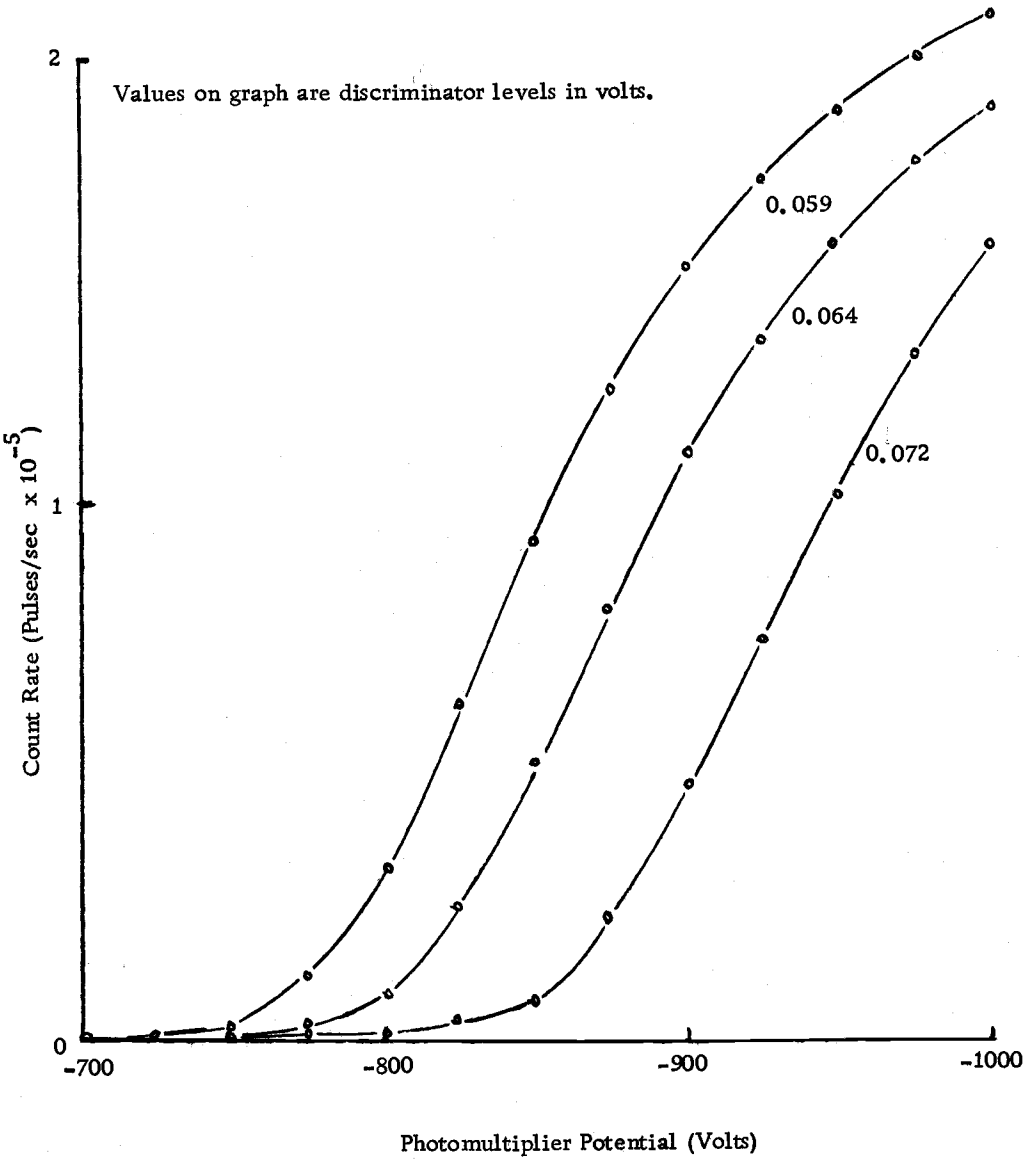

Figure 11. Count rate vs. photomultiplier potential.

photomultiplier voltage fluctuations. The error caused by fluctuation of the photomultiplier potential in a double beam instrument is shown in Table 4. A 1% change in photomultiplier voltage causes only a 0.18% change in readout.

Table 4. Photomultiplier potential instability error for the double beam instrument.

Photomultiplier potential (volts)	Count rate deviation (%)
950	+1.2
925	+0.7
900	0.0
875	-0.4
850	-0.8

Table 5 summarizes the errors caused by various power supply fluctuations in the single and double beam instruments. Regulation is defined here as the percent change in readout caused by a 1% change in voltage. When the power supplies are not purposely changed the average deviation in count for the double beam instrument is 0.1% and for a single beam instrument 0.25%. A larger total count might also give a smaller deviation. More perfectly matched light paths, electronics and photomultiplier tubes would probably help obtain the improved reproducibility the author believes possible with this system.

Table 5. Regulation (Δ Output/ Δ Voltage).

	+12 comparitor voltage	-6 comparitor voltage	Photomultiplier voltage	Counter voltage
Single beam	0.50	0.85	2.2	0.05
Double beam	0.09	0.33	0.18	< 0.05

Dark Current

The dark current or background noise for a digital photometer depends upon several variables. The dark current increases with respect to the total count rate as the photomultiplier potential is increased. It decreases with respect to the total count as the discriminator voltage and/or light intensity increase. The noise pulses can be discriminated against since they are generally small. Their rate is constant at a given photomultiplier potential so an increased count rate diminishes their relative importance. Table 6 reports dark current in counts per second for a range of photomultiplier potentials at several discriminator voltages.

As the light intensity is increased, the total count rate increases and the dark current becomes less prominent. In the case of a double beam instrument when the reference beam controls the counting interval, a faster count rate will reduce the counting time and thus the dark current count. For a photomultiplier potential of 900 volts, a

discriminator level of 0.064 volts and a count rate of 1×10^6 per second, the dark current accounts for about 0.09% of the total count. At a count rate of 2×10^6 per second the dark current value drops by half.

Table 6. Dark current.

Photomultiplier potentials (volts)	Dark current (counts/second) For discriminator levels of 0.060V	0.064V	0.072V
1000	3000	2520	1970
950	1780	1620	1100
900	1260	900	420
850	565	350	155
800	225	91	27
750	32	12	7
700	4	2	1

Dead Time

Figure 12 shows the relationship of the observed count rate to the relative light intensity at various discriminator levels. The hollow cathode light source was used at 20 ma. The photometer was operated as a single beam instrument here. The curves represent the sample beam detection system of the double beam instrument only. The light intensity was varied by placing solutions of varying concentration in the light path. The percent transmittance of each concentration was determined experimentally using the same light source at

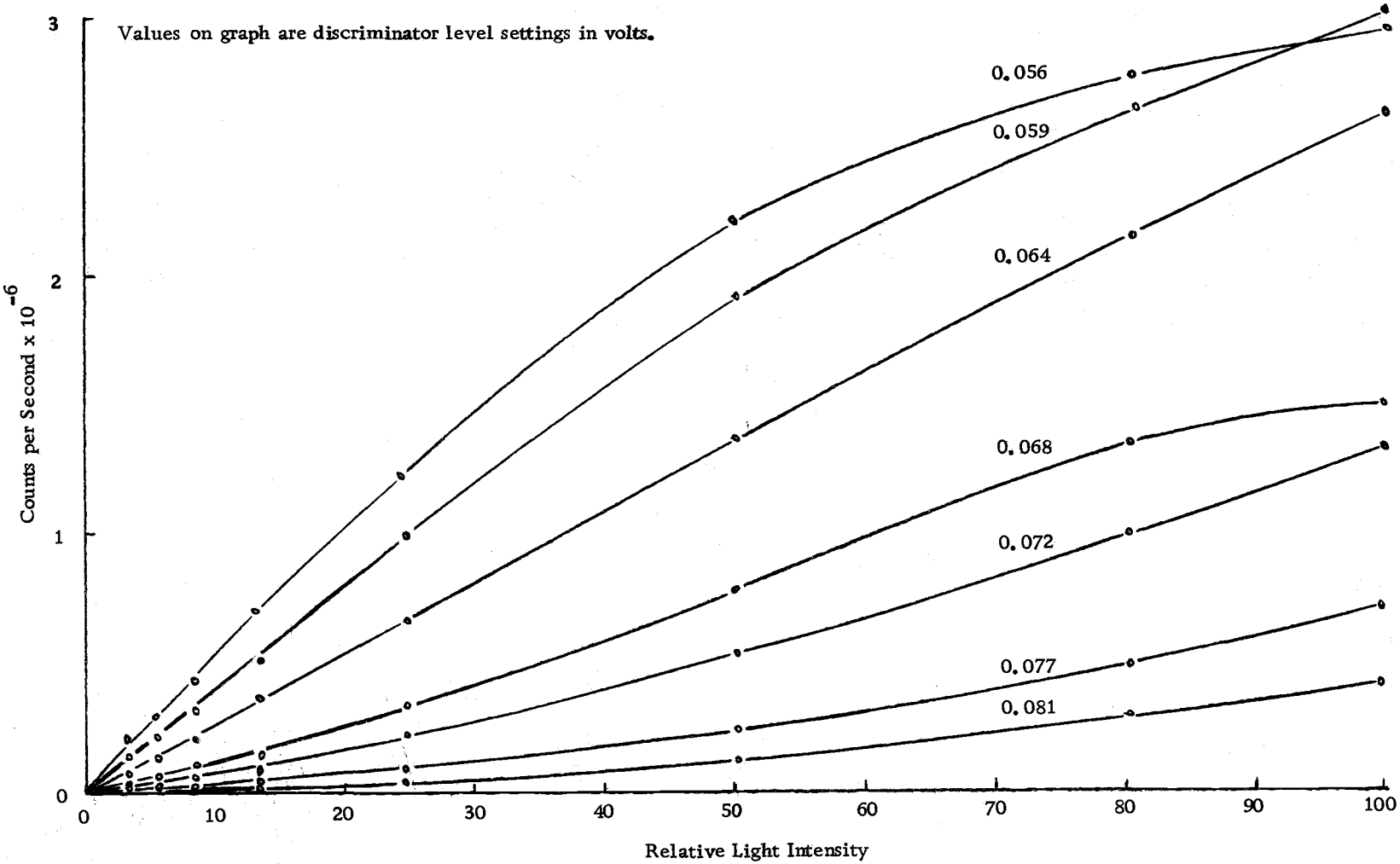

Figure 12. Count rate vs. relative light intensity.

low intensities.

Figure 13 graphs the observed count rate vs. the count rate with an absorber at various discriminator levels. The light intensity was controlled with the adjustable slit. The experimental conditions were the same as in Figure 12. The count rate with an absorber is proportional to the absolute light intensity at a given discriminator level if absorbance is independent of light intensity and if dead time losses are negligible at low count rates.

The plots in Figures 12 and 13 exhibit deviation from linearity in two directions: toward an upward curvature at high discriminator levels and toward a downward curvature at low discriminator levels. At low discriminator levels, the dominant effect is count loss due to pulse overlap at high light levels. This is because at any given light level the lower discriminator voltage is exceeded by more pulses as evidenced by the higher observed counting rates. These more numerous pulses have a greater incidence of overlap. Note that in Figure 12 at low light intensities the count rate is highest for the lowest threshold voltage 0.059 volts, but at higher levels the count loss becomes more pronounced. At high light intensities, the count rate may even fall below that of the next higher discriminator level. At about four million counts per second the count rate begins to decrease with increased light intensity.

The second effect is more prevalent at higher discriminator

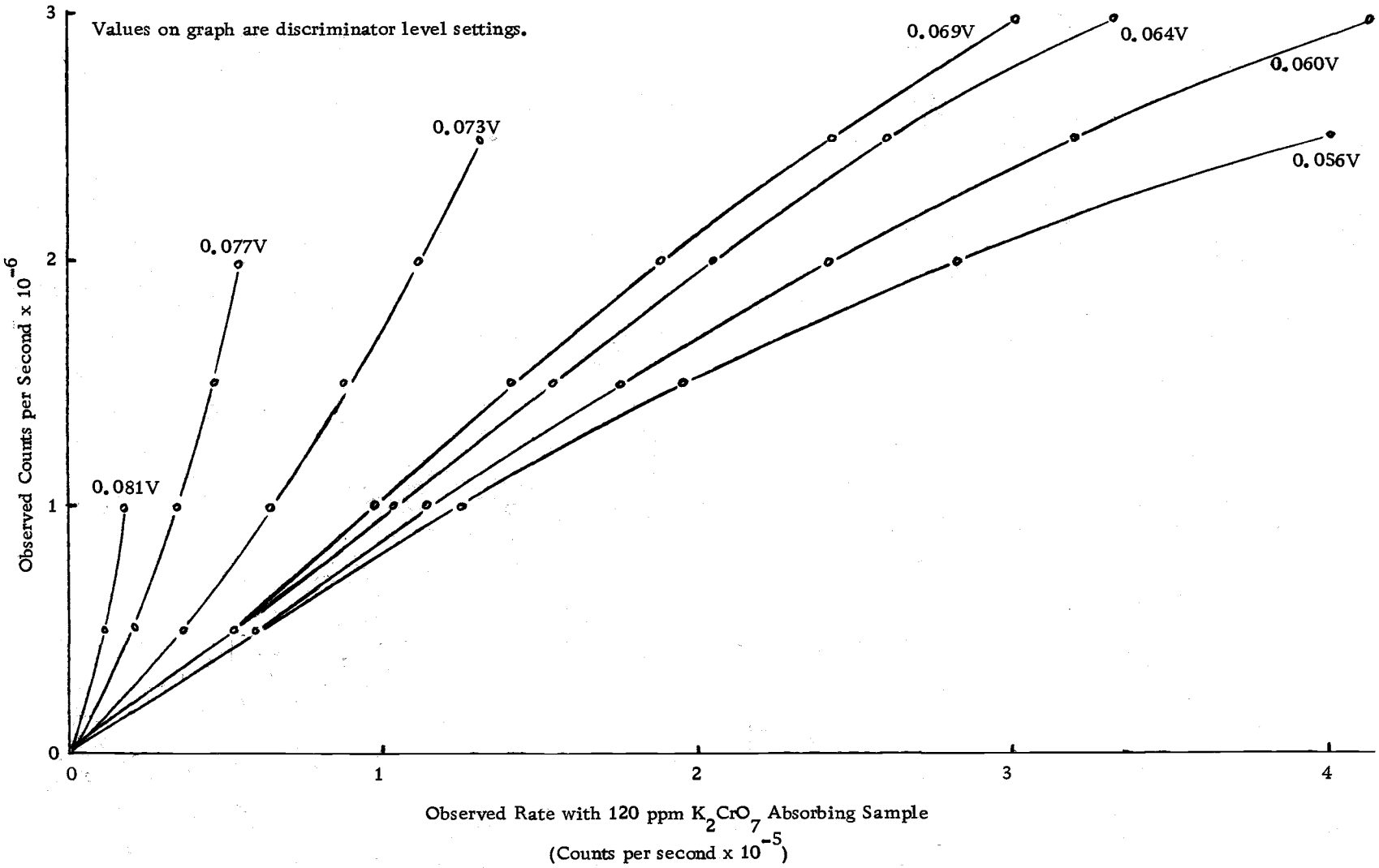

Figure 13. Observed count rate vs. count rate with absorbing sample. Hollow cathode light source at 20 ma.

levels. It causes an increase in count rate greater than would be expected at high light levels. The best explanation is that overlapping of two or more uncountable pulses forms a higher countable pulse. The higher discriminator voltages may be above all but a few pulses but as the light intensity increases, smaller pulses overlap forming larger pulses which may exceed the discriminator voltage. This effect is much more noticeable when the observed count rate without an absorbing sample is graphed against the observed count rate with an absorbing sample which is proportional to true intensity as in Figure 13.

Both effects would be present to some extent at any discriminator level. The 0.068 volt plot in Figure 12 and the 0.069 volt plot in Figure 13 show both effects. Note that the two effects can partially cancel each other as in the 0.064 volt plot which is very nearly linear to 2×10^6 counts per second in both figures.

A discriminator setting of 0.064 volts was chosen as the permanent working level for the sample beam and was used in all further work. The reference beam discriminator setting was adjusted so that the output waveforms matched as close as possible as detected with the Textronics 555 Ocilliscope. Figure 14 shows a plot of the observed count rate vs. the count rate with absorber for the sample beam detector at this discriminator level. The hollow cathode light source was employed at 20 ma. Figure 15 shows a similar plot using

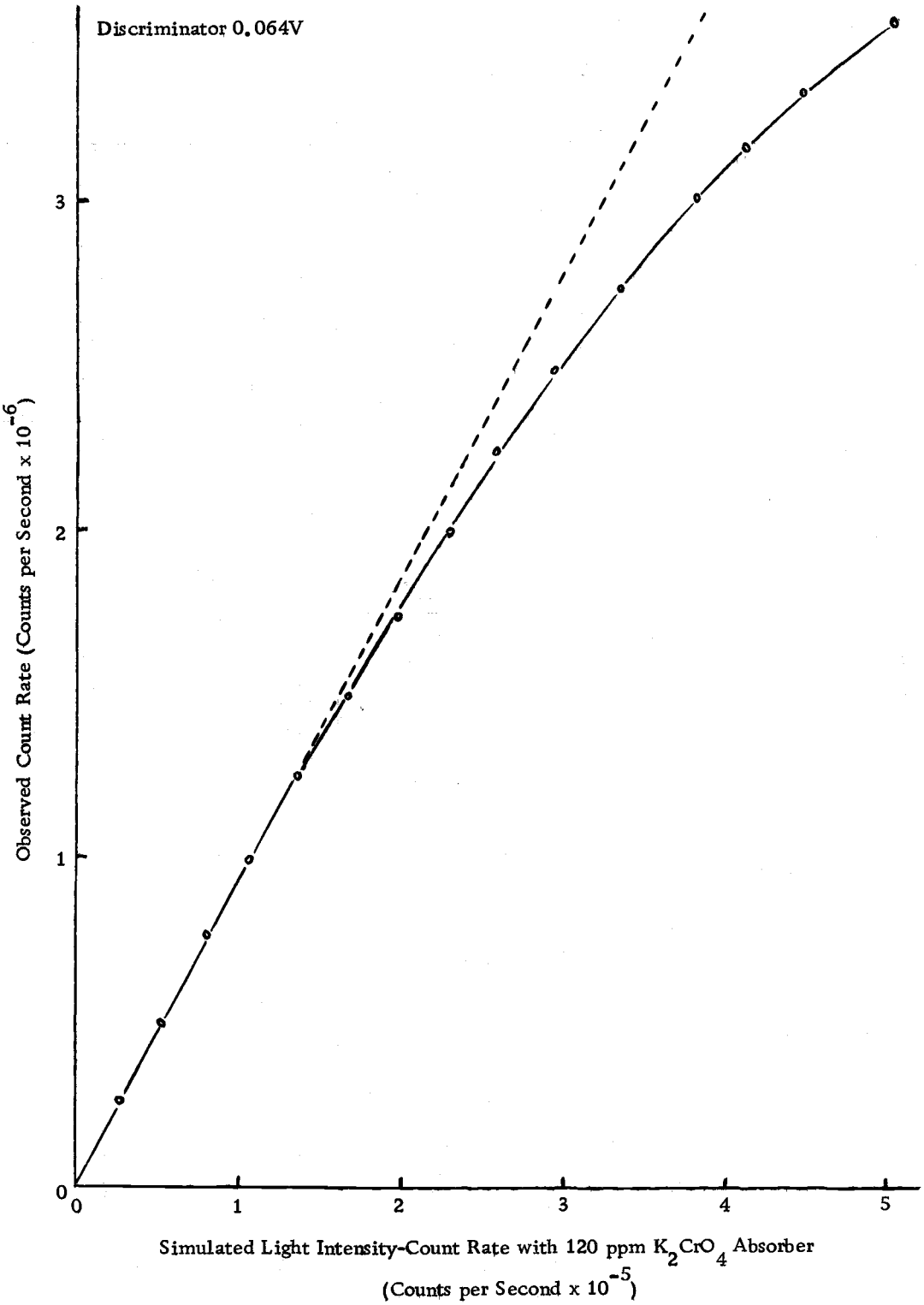

Figure 14. Observed count rate vs. count rate with absorbing sample. Hollow cathode light source at 20 ma.

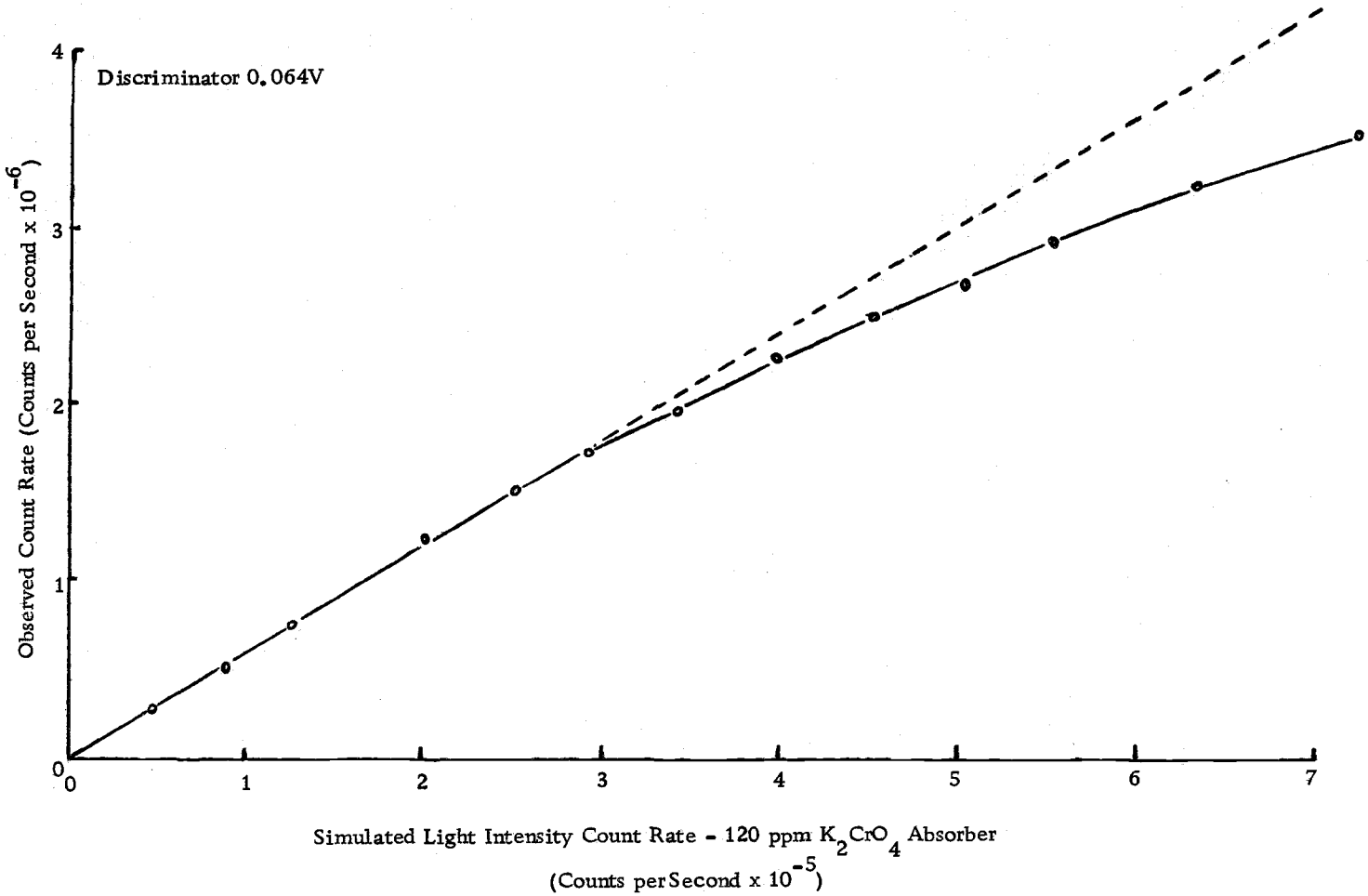

Figure 15. Observed count rate vs. count rate with absorbing sample. Tungsten Bulb Light Source.

the tungsten bulb light source at 3.8 volts. The average dead times were calculated at various observed count rates by the simulated light intensity method described earlier using both Equations 14 and 16. The results are reported in Table 7.

Figures 16 and 17 show plots of the transmittance of the absorber vs. the observed reference beam count rate for the hollow cathode at 12.5 ma and the tungsten bulb at 2.8 V respectively. The light intensity was controlled with the adjustable slit. The photometer was used as a double beam instrument. The dead times calculated from these graphs by the transmittance method using Equations 14 and 16 are reported in Table 8.

The values reported in Tables 7 and 8 assume that there are no perturbing effects shown in Figures 14 through 17 other than the loss due to pulse overlap. This does not appear to be the case. Despite the occurrence of other perturbing effects, corrections can be made fairly accurately at any given light intensity and discriminator level using either Equation 14 and 16.

The actual dead time is not expected to vary with light intensity or count rate. The variation in dead time shown in Tables 7 and 8 is probably due to the interaction of the dead time loss and the additive effect discussed earlier. The actual dead time as determined with a Tektronix 555 Ocilloscope is 120 nanoseconds.

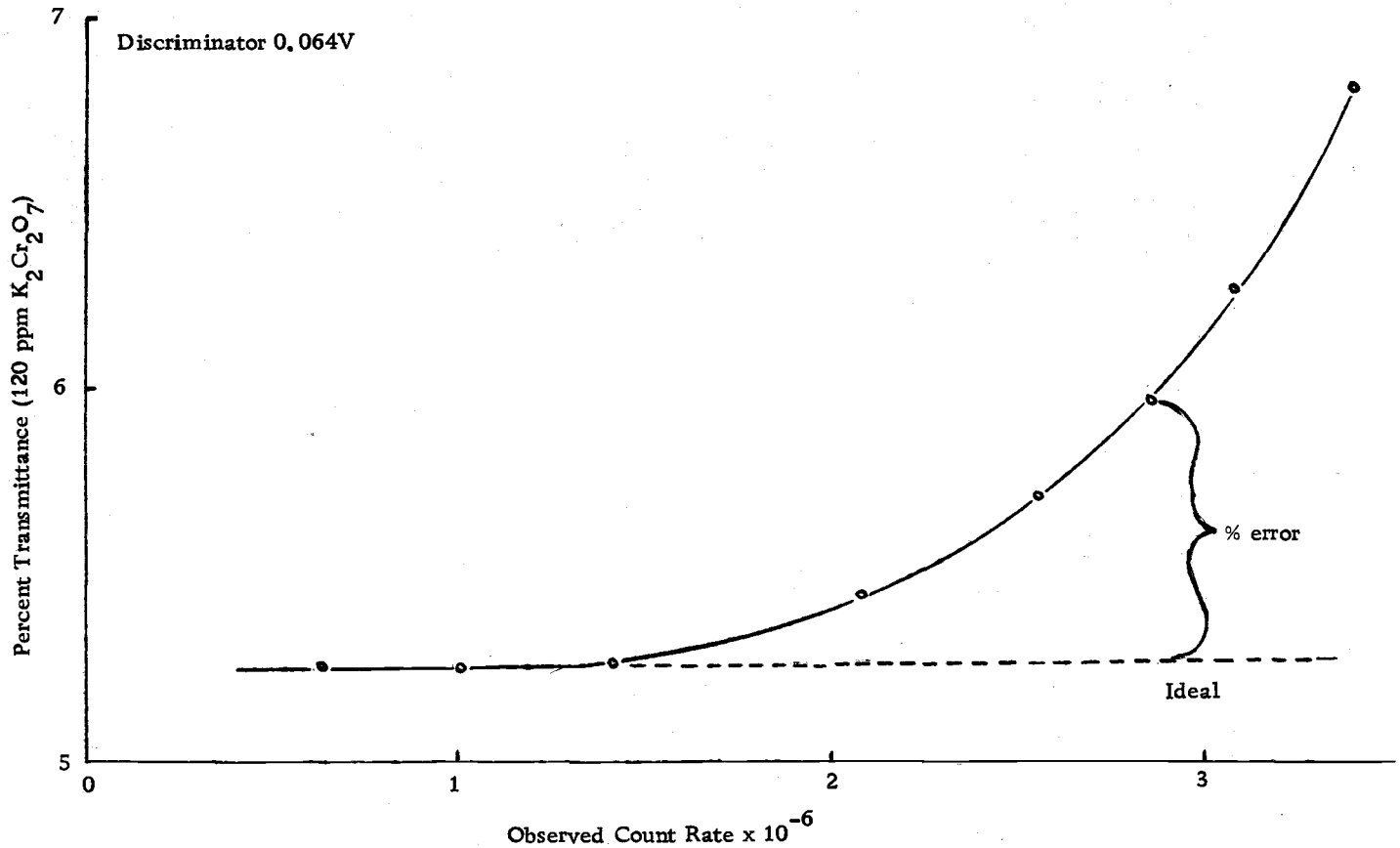

Figure 16. Percent transmittance vs. observed count rate with hollow cathode light source at 12.5 ma.

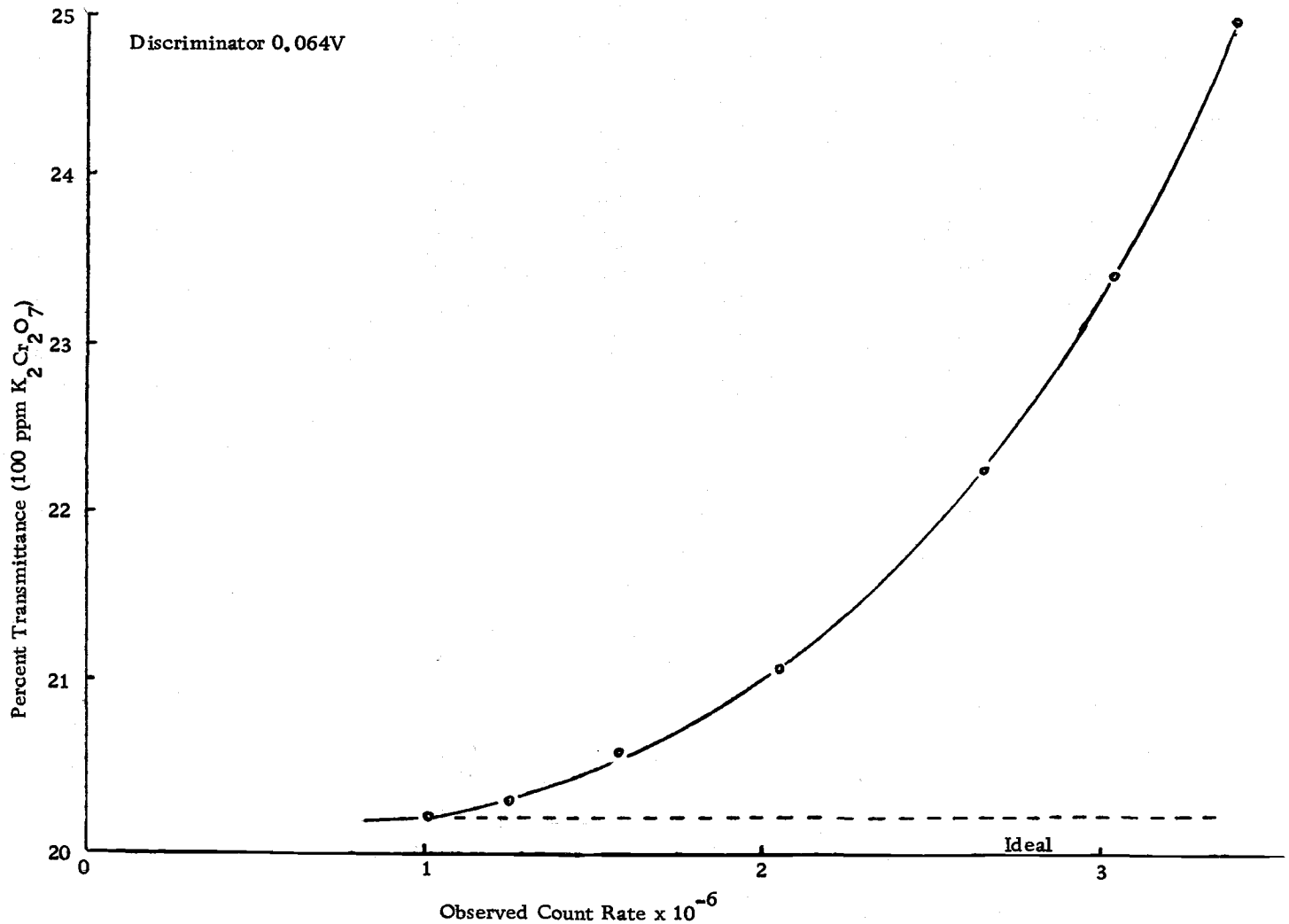

Figure 17. Percent transmittance vs. observed count rate with Tungsten bulb light source at 2.8V.

Table 7. Single beam dead time--simulated light intensity method.

Observed count rate	Calculated dead time (nanoseconds)			
	Equation 14		Equation 16	
	H.C. -20ma	W bulb-3.8V	H.C. -20ma	W bulb-3.8V
1.50×10^6	21	--	21	--
2.00×10^6	24	21	23	21
2.50×10^6	38	31	36	30
3.00×10^6	46	42	43	39

Table 8. Single beam dead time--transmittance method.

Observed count rate	Calculated dead time (nanoseconds)			
	Equation 14		Equation 16	
	H.C. -12.5ma	W bulb-2.8V	H.C. -12.5ma	W bulb-2.8V
2.00×10^6	21	30	21	29
2.50×10^6	33	33	31	31
3.00×10^6	54	46	49	43

Calibration Curves

A series of calibration curves for potassium dichromate at different light intensities are shown in Figure 18. The photometer was used as a double beam instrument. The sample was placed in a sample beam giving a readout directly in percent transmittance. The light intensity was controlled with the hollow cathode current. The reference beam count rates reported correspond to the hollow cathode current as reported below.

H. C. Current (ma)	Count Rate (sec^{-1})
0.35	1.0×10^5
2.0	5.0×10^5
5.5	10.0×10^5
20.0	27.5×10^5

The variation in the plots is due to the more pronounced effects of dead time at higher count rates and the decreasing monochromaticity of the light at higher lamp currents. The deviation from linearity is in part due to a greater count loss in the reference beam than the sample beam caused by the faster count rates of the reference beam. A longer dead time would cause the plot to become nonlinear sooner by increasing the count loss. The higher lamp currents employed to get greater light intensity cause a greater portion of the light to be in the various calcium wavelengths many of which are less strongly absorbed by the dichromate causing a further deviation from linearity.

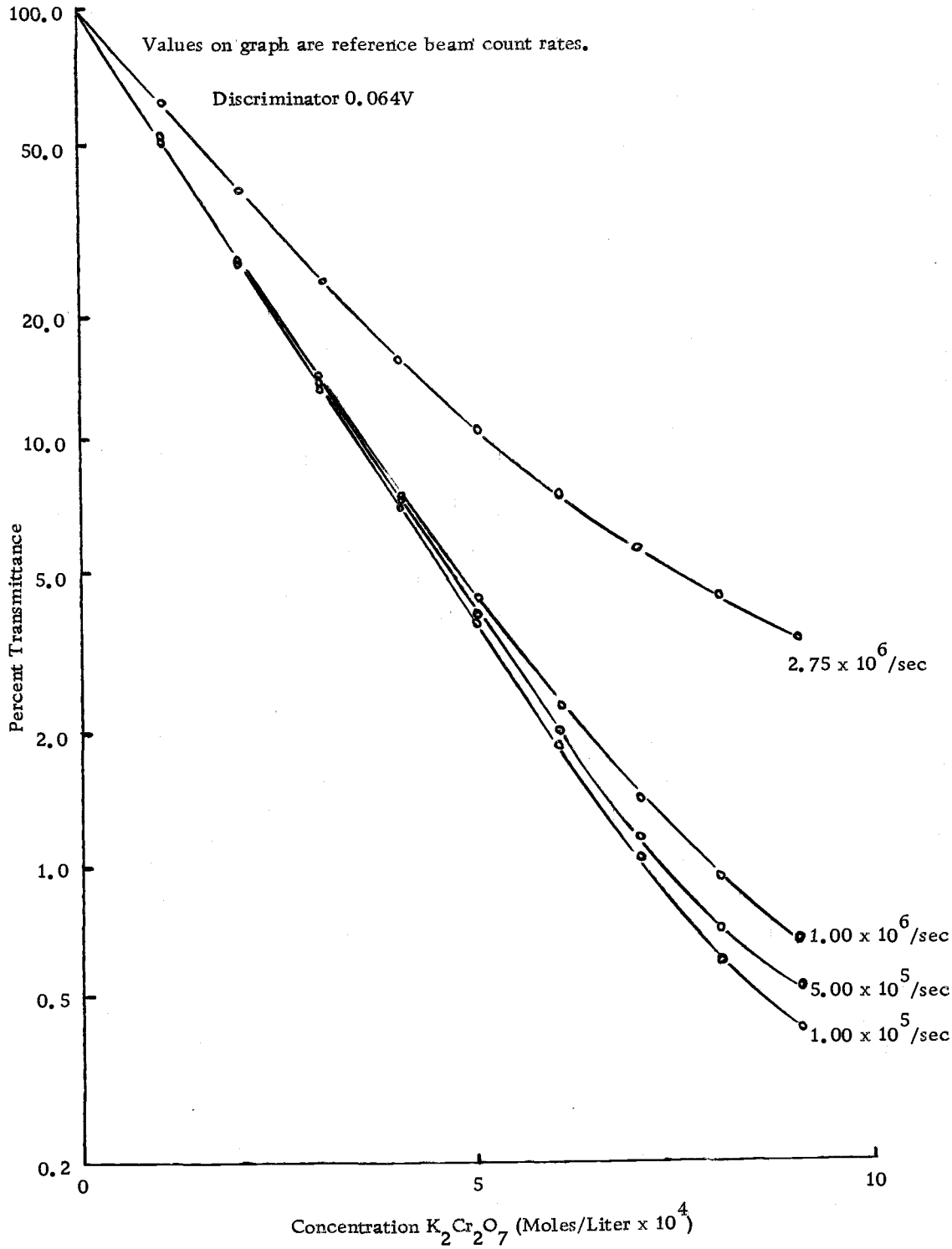

Figure 18. Percent transmittance vs. concentration with hollow cathode light source.

Figure 19 consists of calibration curves for potassium permanganate at different light intensities. The McKee-Pedersen monochromator was used with the exit slit set at 40 microns and the wavelength at 525 nm. Light intensities were changed with the photometer entrance slit. The more monochromatic light of this source allows better agreement of the curves at different counting rates and a better estimation of dead time by count loss as shown by the smaller range of dead times reported in Tables 7 and 8 for the monochromator (W bulb).

Figure 20 is a calibration curve similar to those in Figure 19 except that the sample was placed in the reference cell and the blank in what would ordinarily be the sample cell so that the readout was directly in units of reciprocal transmittance. The count rate was adjusted to 1.00×10^6 counts per second with the adjustable light sources control slit and a blank in both beams. This gives the readout directly in reciprocal transmittance.

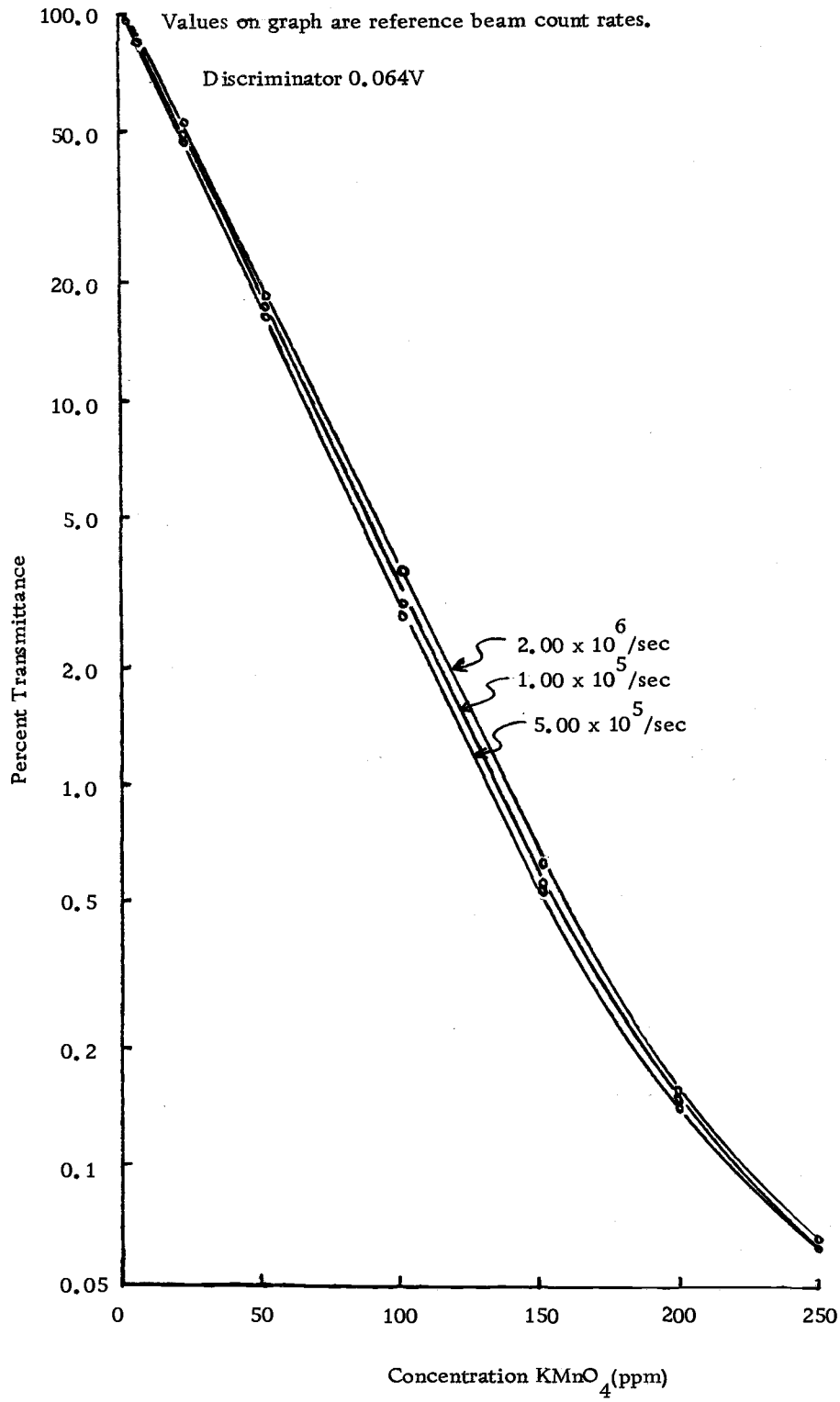

Figure 19. Percent transmittance vs. concentration with Mc Kee-Pedersen light source.

SUMMARY AND CONCLUSIONS

The digital double beam photometer described in this thesis has a short term average deviation of about 0.1% transmittance. This compares favorably with the precision that can be obtained from a quality conventional photometer. A digital photometer built under more rigorous conditions with matched components and a greater counting range would be expected to give greater precision. The digital photometer is cheaper and simpler than quality conventional photometers.

The double beam construction greatly increases the accuracy by reducing count rate dependence on light intensity and power supply fluctuation and provides a method of easy correction for cell and solvent absorption. The digital double beam photometer is more difficult to set because the discriminators must be matched in addition to the light paths and photomultipliers as in conventional photometers.

The data indicates two perturbing effects on pulse counting. The first effect which has been long noted in Geiger-Muller and proportional counters is dead time loss (2). The second effect is a gain in count rate above that expected especially at high discriminator voltages. The explanation offered is that pulses below the discriminator voltage may overlap to form larger pulses which exceed the discriminator voltage.

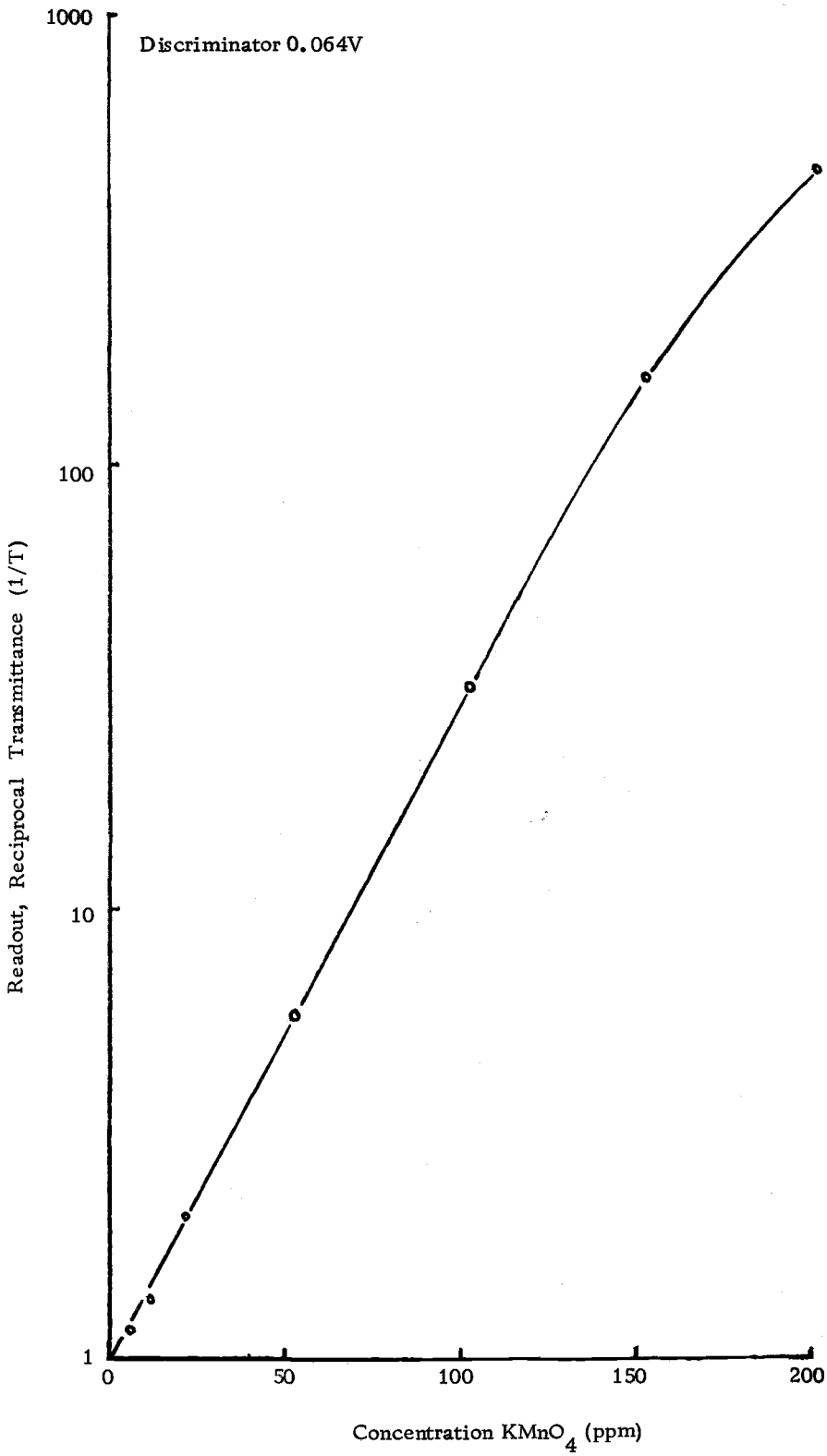

Figure 20. Reciprocal transmittance vs. concentration with Mc Kee-Pedersen light source.

The dead time measured with an oscilloscope was 1.2×10^{-7} seconds, but the effective dead time can be reduced by balancing the two effects mentioned above. This was done by a trial and error adjustment of the discriminator voltage.

The photometer built had a total count limit of 10^6 on both the sample and reference beams. A larger total count limit would be desirable to improve the counting statistics. Since the digital photometer data is reproducible to four significant figures, there is little use in adding more readout counting units per se.

A suggested method of extending the total count limit without adding useless readout counters is to preceed the decade counting units with a variable multidecade dividing unit. The insignificant digits would appear in the MDU which has no readout. The reference dividing unit would be extended to contain the same total number of decades as are in the sample beam. One decade would be added to the readout for each decade in use in the precounting unit divider.

A digital system which is easier to read could be provided using Nixie tubes as described by Solomon (17) rather than numbered bulbs. Such a system is similar in logic to the one used and requires about the same space, but is more expensive. Excellent commercial counters are also available.

Photon counting is most useful at low light intensities and may be employed where extremely low light levels make other photometric

detectors unusable. A suggested use is the spectographic study of dim astronomical objects or faint elemental emission lines.

Part of the purpose of this study concerned the use of newly developed integrated circuits to make a cheaper, simpler photometer. The electrical and optical components cost about $150, excluding the external power supplies. The integrated circuit design allows easy troubleshooting and repair.

BIBLIOGRAPHY

1. Akins, D. L., S. E. Schwartz and C. Bradley Moore. Pulse-to-analog converter for optimizing signal-to-noise from photomultipliers at low light intensities. The Review of Scientific Instruments 39(5): 715-718. 1968.

2. Chase, Grabton D. and Joseph L. Rabinowitz. Principles of Radio-isotope Methodology. Minneapolis, Burgess, 1959. 372p.

3. Cotton, F. Albert and Geoffrey Wilkinson, F. R. S. Advanced Inorganic Chemistry, 2d ed. New York, Interscience, 1966. 1136p.

4. DeLotto, I., P. F. Manfredi and P. Principi. Counting statistics and dead time losses. Energia Nucleare 11(10): 555-564. 1964.

5. Fairchild Semiconductor Manual. 1965.

6. Franklin, M. L., Gary Horlick and H. V. Malmstadt. Basic and practical considerations in utilizing photon counting for quantitative spectrochemical methods. Analytical Chemistry 41(1): 2-10. 1969.

7. Friedlander, Gerhart, Joseph W. Kennedy and Julian M. Miller. Nuclear and radiochemistry. 2d ed. New York, John Wiley & Sons, 1955. 585p.

8. Lancaster, D. Low cost counting unit. Popular Electronics 28(2): 27-32. 1968.

9. Lancaster, D. Ultra-fast electronic stopwatch. Popular Electronics 28(3): 27-34, 92-93. 1968.

10. Muller, R. H. Precision photometry. Analytical Chemistry 37(10): 123A-125A. 1965.

11. Nakamura, J. K. and S. E. Schwarz. Synchronous detection vs. pulse counting for sensitive photomultiplier detection systems. Applied Optics 7(6): 1073-1078. 1968.

12. Pardue, Harry L. and Stanley N. Deming. High-stability low-noise precision spectrometer using optical feedback. Analytical Chemistry 41(7): 986-989. 1969.

13. Piepmeier, Edward H., Donald E. Braun, and Roxie R. Rhodes. A precision photometer using milliwatt light sources and photon counting. Analytical Chemistry 40(11): 1667-1671. 1968.

14. Rainwater, L. J. and C. S. Wu. Applications of probability theory to nuclear detection. Nucleonics 1(2): 60-69. 1947.

15. RCA Photo and Image Tubes Manual. ICE-269.

16. Ross, Harley H. New concept in precision photometric analysis using a radioisotopic light source. Analytical Chemistry 38(3): 414-420.

17. Solomon, Leslie and Alexander W. Burawa. All-purpose nixie readout. Popular Electronics 29(5): 67-71. 1968.

APPENDIX

APPENDIX

Any pulse counting device will have a dead time (recovery time or resolving time) after each recorded pulse during which it is insensitive to other pulses. Two methods have been suggested by Rainwater (14) to calculate this value. They are summarized below.

Let n = the observed count rate,
N = the actual count rate, and
τ = the dead time.

There will be n pulses counted per second having an average insensitive period of τ. The total dead time will then be $n\tau$. Since the total number of pulses emitted per second is N, the number lost will be $nN\tau$. The number of counts lost is the difference between actual pulses and counted pulses of $N-n$. Since these two expressions are equal, we can write the equation:

$$N - n = nN\tau. \tag{13}$$

Solving for τ.

$$\tau = (N-n)/nN \tag{14}$$

The above equation assumes that any pulse occurring during an insensitive period will not lengthen that period. If it is assumed that the insensitive period is extended by τ after the undetected pulse arrives, a different relationship is required. The system will remain blocked if the input pulses are spaced less than τ. A count is obtained whenever a time greater than τ occurs between pulses. Thus

n = N x (probability of zero pulses during the time τ after a given pulse). Since the number of expected counts during time τ is $N\tau$, the probability of no counts is given by $e^{-n\tau}$ and the equation becomes

$$n = Ne^{-N\tau}. \tag{15}$$

Solving for τ.

$$\tau = \ln(N/n)/N. \tag{16}$$

A more detailed mathematical derivation is presented by Delotto (4)

Rainwater's dead time equations take into account only the pulses lost due to overlap. A dead time equation which also takes into account the pulses gained through overlap is developed below.

In a photon counting system, a certain number of pulses (N) are developed per time unit, depending mostly on light intensity and instrument geometry. Of these, a certain fraction (A) will have pulse heights greater than the discriminator voltage and a fraction (1-A) will have pulse heights less than the discriminator voltage. The values of A and (1-A) will depend upon the type of photomultiplier tube, photomultiplier potential, and the discriminator voltage.

The number of natural pulses exceeding the discriminator voltage will be AN, the number not exceeding it will be (1-A)N. Some of the latter will overlap, creating larger pulses. The number of these that overlap may be expressed as the total pulses below the discriminator level minus the ones which do not overlap or

$$(1-A)N - (1-A)Ne^{-(1-A)N\tau} \tag{17}$$

which can be reduced to

$$(1-A)N\,[\,1-e^{-(1-A)N\tau}\,] \tag{18}$$

where τ = the dead time.

A fraction, C, of the overlapping pulses will become large enough to exceed the discriminator voltage so the total number of pulses exceeding the discriminator level will be:

$$AN + (1-A)CN[\,1-e^{-(1-A)N\tau}\,] \tag{19}$$

Using Equation 15 to correct for pulses lost due to dead time we get:

$$n = \{\,AN + (1-A)CN[\,1-e^{-(1-A)N\tau}\,]\,\}\; e^{-\{AN + (1-A)CN[\,1-e^{-(1-A)N\tau}\,]\}\,\tau} \tag{20}$$

where n = the observed pulse rate. Determining proper values for all of the unknowns in this equation may prove difficult but if it is done a better fit to the experimental curve should be obtained.